Neurobiology of Disease

IL-4 Signaling Drives a Unique Arginase$^+$/IL-1β^+ Microglia Phenotype and Recruits Macrophages to the Inflammatory CNS: Consequences of Age-Related Deficits in IL-4Rα after Traumatic Spinal Cord Injury

Ashley M. Fenn,[1] Jodie C.E. Hall,[1] John C. Gensel,[2] Phillip G. Popovich,[1,3,4] and Jonathan P. Godbout[1,3,4]

[1]Department of Neuroscience, The Ohio State University, Columbus, Ohio 43210, [2]Spinal Cord and Brain Injury Research Center, the University of Kentucky, Lexington, Kentucky 40536, and [3]Center for Brain and Spinal Cord Repair and [4]Institute for Behavioral Medicine Research, The Ohio State University, Columbus, Ohio 43210

Alternative activation of microglia/macrophages (M2a) by interleukin (IL)-4 is purported to support intrinsic growth and repair processes after CNS injury. Nonetheless, alternative activation of microglia is poorly understood *in vivo*, particularly in the context of inflammation, injury, and aging. Here, we show that aged mice (18–19 months) had reduced functional recovery after spinal cord injury (SCI) associated with impaired induction of IL-4 receptor α (IL-4Rα) on microglia. The failure to successfully promote an IL-4/IL-4Rα response in aged mice resulted in attenuated arginase (M2a associated), IL-1β, and chemokine ligand 2 (CCL2) expression, and diminished recruitment of IL-4Rα^+ macrophages to the injured spinal cord. Furthermore, the link between reduced IL-4Rα expression and reduced arginase, IL-1β, and CCL2 expression was confirmed using adult IL-4Rα knock-out (IL-4Rα^{KO}) mice. To better understand IL-4Rα-mediated regulation of active microglia, a series of studies was completed in mice that were peripherally injected with lipopolysaccharide and later provided IL-4 by intracerebroventricular infusion. These immune-based studies demonstrate that inflammatory-induced IL-4Rα upregulation on microglia was required for the induction of arginase by IL-4. In addition, IL-4-mediated reprogramming of active microglia enhanced neurite growth *ex vivo* and increased inflammatory gene expression (i.e., IL-1β and CCL2) and the corresponding recruitment of CCR2$^+$/IL-4Rα^+/arginase$^+$ myeloid cells *in vivo*. IL-4 reprogrammed active microglia to a unique and previously unreported phenotype (arginase$^+$/IL-1β^+) that augmented neurite growth and enhanced recruitment of peripheral IL-4Rα^+ myeloid cells to the CNS. Moreover, this key signaling cascade was impaired with age corresponding with reduced functional recovery after SCI.

Key words: **advanced age; IL-4; inflammation; M2a; microglia; spinal cord injury**

Introduction

Alternative activation of microglia/macrophages (M2a) is purported to be protective after spinal cord injury (SCI) participating in intrinsic survival, growth, and repair processes (David and Kroner, 2011). Nonetheless, the M2a phenotype is poorly understood *in vivo* and recent studies indicate that it may be impaired with normal aging (Fenn et al., 2012; Lee et al., 2013). Impaired M2a microglial regulation may explain why older individuals (60+ years) have reduced functional recovery and increased mortality after a traumatic injury to the brain or spinal cord (Chen et al., 1997; Onyszchuk et al., 2008; National SCI Statistical Center, 2013). Indeed, in rodent models of traumatic brain injury, a worse functional outcome in the aged corresponded with reduced IL-4 signaling (Kumar et al., 2013) and increased CNS inflammation (Sandhir et al., 2008). Few studies, however, have investigated a mechanism for increased age-associated morbidity and mortality after SCI. This is a significant problem because incidence of SCI in aged individuals has increased fivefold in the last 30 years and currently comprises 15% of SCI cases each year (Fassett et al., 2007). Thus, a better understanding of how different microglia/macrophage phenotypes affect SCI recovery in the aged is required.

Understanding of distinct microglia/macrophage phenotype has expanded within the last decade. Unfortunately, M1, M2a, M2b, and M2c phenotyping has primarily been done *in vitro* and whether or not these distinct phenotypes develop *in vivo* and what functions they perform are not well defined (Mosser and

Received March 21, 2014; revised May 8, 2014; accepted May 28, 2014.

Author contributions: A.M.F., J.C.E.H., J.C.G., P.G.P., and J.P.G. designed research; A.M.F., J.C.E.H., and J.C.G. performed research; J.C.G., P.G.P., and J.P.G. contributed unpublished reagents/analytic tools; A.M.F. and J.P.G. analyzed data; A.M.F., J.C.E.H., P.G.P., and J.P.G. wrote the paper.

This research was supported by National Institute on Aging Grant R01-AG-033028 to J.P.G. A.M.F. was supported by a Med into Grad Fellowship from the Howard Hughes Medical Institute and is currently supported by an Ohio State Presidential Fellowship. We thank Zhen Guan (Ohio State University, OSU), Yan Huang (OSU), and Dr. Nicole Powell (OSU) for their technical assistance.

The authors declare no competing financial interests.

Correspondence should be addressed to J.P. Godbout, 259 IBMR Building, 460 Medical Center Drive, The Ohio State University, Columbus, OH 43210. E-mail: jonathan.godbout@osumc.edu.

DOI:10.1523/JNEUROSCI.1146-14.2014

 0270-6474/14/348904-14$15.00/0

Edwards, 2008). In the context of SCI, the IL-4-driven M2a phenotype has received the most attention because it may support a level of endogenous repair (David and Kroner, 2011). For example, in models of nerve and spinal cord injury, increased expression of the M2a marker arginase was associated with prolonged axonal protection (Barrette et al., 2010) and improved neuronal growth and survival (Cao et al., 2005). Moreover, media from IL-4-treated macrophages enhanced neurite growth *in vitro* (Kigerl et al., 2009). Thus, an inability to respond to IL-4/IL-13 and induce an M2a phenotype after SCI may impede functional recovery in the aged.

Therefore, the aims of this study were twofold: (1) test the hypothesis that impaired IL-4Rα induction and M2a regulation of microglia in the aged CNS results in an attenuated microglial response and worse functional outcome after SCI and (2) better characterize the M2a phenotype *in vivo* in the context of SCI and inflammation. We show novel data that aged mice had reduced functional recovery after SCI associated with failed induction of IL-4Rα and reduced M2a responses in microglia (reduced arginase), but also reduced inflammatory cytokine (IL-1β) and chemokine (CCL2) expression necessary to recruit IL-4Rα$^+$ monocytes/macrophages to the injured spinal cord. Moreover, evidence from immune-based studies shows that induction of IL-4Rα on microglia was required for IL-4-dependent arginase expression *in vivo* and axon outgrowth *ex vivo*. Last, inflammatory-activated microglia reprogrammed with IL-4 *in vivo* increased expression of IL-1β mRNA associated with heightened CCL2 in the brain and enhanced recruitment of CCR2$^+$/IL-4Rα$^+$/Arg$^+$ myeloid cells to the CNS.

Materials and Methods

Mice. Adult BALB/c mice were obtained from a breeding colony kept in barrier-reared conditions in a specific pathogen-free facility at The Ohio State University. A breeding colony was established for adult IL-4Rα-deficient (IL-4Rα^{KO}) mice on a BALB/c background (BALB/c-*Il4ra*^{tm1Sz}/J; #003514). Breeding pairs were purchased from Jackson Laboratories. Adult C57BL/6 mice were purchased from Charles River Breeding Laboratories, adult C57BL/6-Tg$^{(CAG-EGFP)}$ 131/leysopJ mice (#006567) were purchased from The Jackson Laboratory, and aged BALB/c mice (18–22 months) were purchased from the National Institute on Aging specific pathogen-free colony (maintained at Charles River Laboratories). Mice were individually housed in polypropylene cages and maintained at 25°C under a 12 h light/dark cycle with *ad libitum* access to water and rodent chow. All procedures were in accordance with the National Institute of Health Guidelines for the Care and Use of Laboratory Animals and were approved by The Ohio State University Institutional Laboratory Animal Care and Use Committee.

SCI. SCI was performed as previously described (Jakeman et al., 2000; Donnelly et al., 2011). In brief, mice were deeply anesthetized using ketamine and xylazine (100 and 10 mg/kg BW i.p., respectively) and received a laminectomy at vertebral level T9 or a laminectomy followed by a spinal cord contusion using the Infinite Horizons device (75 kdyn; Precision Systems and Instrumentation). Mice were returned to a slide-warmed cage (35−37°C) with three to four mice per cage and administered 2 ml sterile saline, and 100 μl Gentocin (5 ml/kg) subcutaneously. Mice were maintained on the slide-warmed cage overnight. Mice receiving a spinal cord contusion underwent bladder expression twice daily for the duration of the experiment.

Motor recovery. Basso Mouse Scale (BMS) scoring was completed as previously described (Basso et al., 2006). In brief, mice were acclimated to a plastic-bottomed open field (100 cm diameter, 21 cm wall height) every other day for 1 week before injury. Because BALB/c mice freeze in an open field under bright light, dim light was used for all BMS testing. After injury mice were placed individually in the open field 1, 3, 5, 7, 14, 21, and 28 d post injury (dpi). During testing mice were scored for 4 min by two observers blinded to experimental treatment. Mice were rated by on a scale of 0–9. Testing was completed during the light phase at the same time each day.

Purification of enriched microglia from brain. Enriched microglia were isolated from brain as previously described (Henry et al., 2009; Fenn et al., 2012). In brief, the brain was homogenized through a 70 μm cell strainer and centrifuged to collect a cell pellet. Cells were then suspended in a discontinuous Percoll density gradient (70%/50%/35%/0%) and centrifuged. Microglia and peripherally derived CD11b$^+$ cells were collected at the 70%/50% Percoll interphase (Henry et al., 2009; Wohleb et al., 2012). In these studies, Percoll-isolated cells were primarily microglia. For example, Percoll-isolated cells from control mice (Saline-Veh, Saline-IL-4) were ~78% CD11b$^+$/CD45^{lo} microglia and ~3% CD11b$^+$/CD45^{hi} peripherally derived macrophages and granulocytes. Following lipopolysaccharides (LPS; LPS-Veh, LPS-IL-4) the percentage shifted to ~75% microglia and ~9% peripherally derived macrophages and granulocytes. Based on these percentages, Percoll-isolated cells from the brain are referred to as "enriched microglia."

Purification of enriched CD11b$^+$ cells from spinal cord. Enriched CD11b$^+$ cells were isolated from the spinal cord as previously described (Donnelly et al., 2011). In brief, the entire spinal cord was homogenized through a 70 μm cell strainer and centrifuged to collect a cell pellet. Cells were then suspended in a modified discontinuous Percoll density gradient (70%/35%/0%) and centrifuged. Microglia and peripherally derived CD11b$^+$ cells were collected at the 70%/35% Percoll interphase. Because of this modified gradient, a larger proportion of isolated cells was not of a CD11b$^+$ lineage and likely consisted of other brain glia including astrocytes (Norden et al., 2014). Nonetheless, in these studies Percoll-isolated cells from laminectomy mice were ~58% CD11b$^+$/CD45^{lo} microglia, ~2% CD11b$^+$/GR1$^{lo/neg}$ macrophages, and ~1.5% CD11b$^+$/GR1^{hi} granulocytes. Following SCI the percentage shifted to ~43% microglia, ~6% macrophages, and ~6% granulocytes. Because of the lower proportion of microglia isolated from the spinal cord and increase in peripherally derived cells, Percoll-isolated cells from the spinal cord are referred to as "enriched CD11b$^+$ cells."

Intracerebroventricular cannulation and injections. Intracerebroventricular cannulation was performed as previously described (Huang et al., 2008). In brief, mice were deeply anesthetized using ketamine and xylazine (100 and 10 mg/kg BW i.p., respectively). A 26 gauge stainless steel guide cannula was placed in the lateral cerebral ventricle using the following stereotaxic coordinates from bregma: Lateral 1.2 mm; A-P 0.5 mm; and a depth of −2 mm from the dura mater. Two anchoring cranial screws were inserted adjacent to the cannula and the cannula was secured with cranioplastic cement. A dummy cannula was inserted in the guide cannula to prevent occlusion and infection. Mice were injected subcutaneously with Buprenex (111 μg/kg BW) after surgery and again 24 h later. Mice were provided a minimum of 7 d to recover before treatment.

After at least 7 d post intracerebroventricular cannulation, mice were given an intraperitoneal injection of saline or LPS (0.33 mg/kg–BALB/c; 0.5 mg/kg–C57BL/6). One hour later mice received a 2 μl volume intracerebroventricular injection of vehicle (0.1% BSA) or IL-4 (25 ng/μl) at a rate of 1 μl/min. Twenty-four hours after LPS injection mice were killed or perfused and brains were collected for flow cytometric, RNA, or immunohistochemical analyses.

DRG neuronal cultures with microglia. For the DRGs, cervical, thoracic, and lumbar DRG neurons were isolated from the spinal cord as described previously (Gensel et al., 2009). In brief, DRGs were dissected from an adult BALB/c mouse spinal cord and plated at a density of 800 cells/well in a 24-well plate and maintained in fresh media (Neurobasal A with 2% B27 supplement (Invitrogen), 1% GlutaMAX, and 1% penicillin/streptomycin) at 37°C/5% CO_2 for 3 d before treatment. After 3 d, a separate subset of adult BALB/c mice was injected with saline or LPS intraperitoneally. After 4 h microglia were isolated by Percoll gradient separation and added at a density of ~1×10^5 cells/well to 0.4 μm transwell inserts situated directly above DRG neurons. Microglia/DRG cocultures were then treated with vehicle (0.1% BSA) or IL-4 (20 ng/ml) for 24 h.

GFP$^+$ bone marrow-chimera. Bone marrow (BM)-chimeras were established using chemical ablation with busulfan and reconstitution of the BM with donor cells obtained from C57BL/6-Tg$^{(CAG-EGFP)}$ mice as previously described (Wohleb et al., 2013). In brief, recipient C57BL/6 male

mice (6 weeks old) were injected intraperitoneally once daily for 2 consecutive days with busulfan in a 1:1 solution of DMSO and deionized H_2O (30 mg/kg/100 μl). Donor C57BL/6-$Tg^{(CAG-EGFP)}$ BM-derived cells were isolated from the femur, passed through a 70 μm cell strainer, and the total number of cells was determined with a BD Coulter Particle Count and Size Analyzer (Beckman Coulter). Donor BM-derived cells (1×10^6) were transferred to recipient mice by tail vein injection (100 μl) 48 h after the second dose of busulfan. Mice were left undisturbed for 4 weeks to allow for engraftment. Engraftment was verified by determining the percentage of GFP^+ cells in the BM and the blood. Mice that had <30% BM engraftment were excluded from the study.

RNA isolation and RT-PCR. RNA was isolated from a 1 mm coronal brain section or two, 1 mm spinal cord sections immediately adjacent to the injury epicenter using the Tri-Reagent protocol (Sigma) and subjected to the DNA-free RNA clean up procedure (Ambion) according to manufacturer instructions. RNA was isolated from Percoll-enriched microglia or $CD11b^+$ cells using the PrepEase kit (Affymetrix) according to manufacturer's instructions. Real-time (RT)-PCR was performed using the Applied Biosystems TaqMan Assays-on-Demand Gene Expression protocol as previously described (Wohleb et al., 2011, 2012). In brief, experimental cDNA was amplified by RT-PCR where a target cDNA (e.g., IL-1β, arginase I, CCL2) and a reference cDNA (GAPDH) were amplified simultaneously using an oligonucleotide probe with a 5′ fluorescent reporter dye (6-FAM). Fluorescence was determined on an ABI PRISM 7300 sequence detection system (Applied Biosystems). Data were analyzed using the comparative threshold cycle method and results are expressed as fold difference from GAPDH.

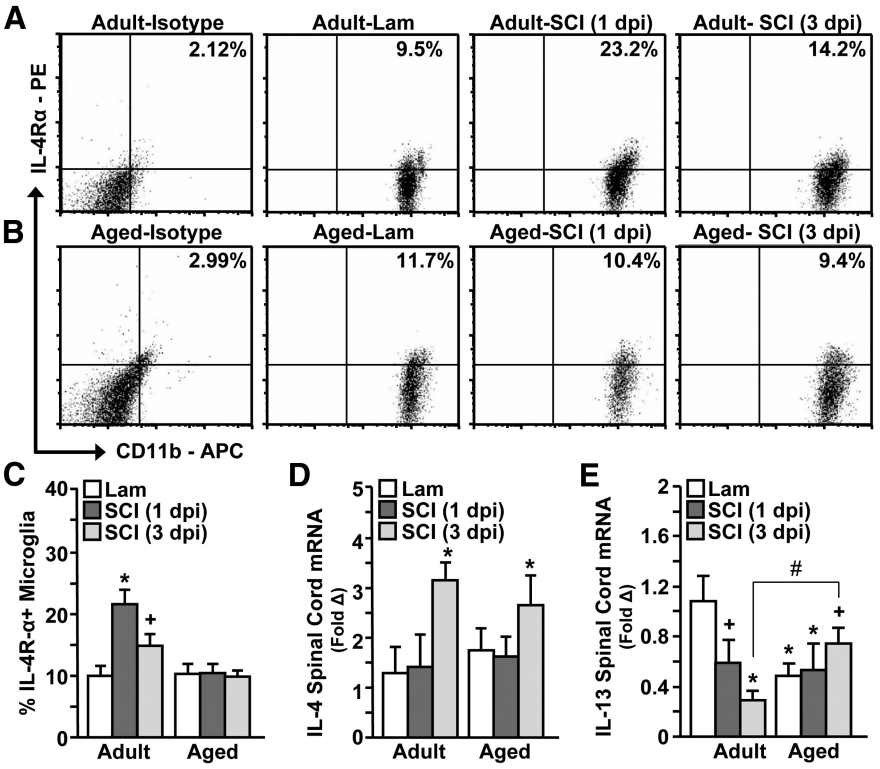

Figure 1. Age-related impairment in the induction of IL-4Rα surface expression on microglia after SCI. Adult female (3–4 months) and aged female (18–22 months) BALB/c mice were subjected to a mid-thoracic (T9) laminectomy (Lam) or SCI. After 1 dpi or 3 dpi, enriched $CD11b^+$ cells from the spinal cord were isolated. Representative bivariate dot plots of CD11b/IL-4Rα labeling in microglia from (***A***) adult and (***B***) aged mice. Gating was based on age-matched isotype controls. ***C***, Average percentage of IL-4Rα$^+$ microglia ($n = 4–5$). ***D***, IL-4 and (***E***) IL-13 mRNA expression was determined from two 1 mm sections of spinal cord collected adjacent to the lesion epicenter ($n = 4–5$). Error bars represent the mean ± SEM. Means with $^*p < 0.05$ are significantly different and means with $^+p = 0.1$ tend to be different from Adult-Lam controls. Means with $^\#p < 0.05$ are significantly different from Adult-SCI-3 dpi.

Flow cytometry. Cells were assayed for surface antigens by flow cytometry as previously described (Henry et al., 2009; Fenn et al., 2013). In brief, Percoll-enriched microglia or $CD11b^+$ cells were incubated with rat anti-mouse CD14-FITC, CD11b-PE, CD45-PerCP-Cy5.5, and CCR2-APC antibodies (eBioscience). For the GFP chimera experiments, cells were fluorescent for GFP (FITC + PE channels) and incubated with CD45-PerCP-Cy5.5 and CD11b-APC antibodies. Expression of these surface receptors was determined using a BD FACSCalibur four-color cytometer. Ten thousand events characterized as microglia/macrophages were recorded. Microglia and macrophages were identified by $CD11b^+/CD45^{lo}$ and $CD11b^+/CD45^{hi}$ expression, respectively (Wohleb et al., 2011). For each antibody, gating was determined based on appropriate negative isotype-stained controls. Flow data were analyzed using FlowJo software (Tree Star).

Immunohistochemical staining. Mice were killed by CO_2 and transcardially perfused with 0.1 M PBS followed by 4% formaldehyde. Tissues were cryoprotected with 30% sucrose for 72 h following postfixation. For all tissues three representative images from each sample were taken for analysis. Fluorescent images were taken with a Zeiss 510 Meta confocal microscope and analyzed using MetaMorph Analysis software (Molecular Devices). DAB/eriochrome cyanine (EC) images were taken with a Carl Zeiss Axioplan 2 Imaging microscope and analyzed using ImageJ NIH software.

Spinal cord. spinal cords were rapidly frozen in OCT compound. Serial coronal sections (10 μm) were cut using a Microm HM550 cryostat (Mikron Instruments) and collected every 100 μm throughout a 5 mm segment with the lesion epicenter at the middle. Sections were stained with antibodies against arginase I (1:200; Santa Cruz Biotechnology) and Tomato lectin (TomL; 1:200; Sigma; Kigerl et al., 2006) for fluorescent staining, or neurofilament (1:1000; Aves Labs), and EC (Sigma) solution for DAB staining. For measuring epicenter tissue sparing, images were taken at the epicenter and up to 200 μm rostral and caudal of the epicenter.

Brain. Brains were frozen in dry-ice cooled isopentane. Coronal sections (10 μm) were cut using a Microm HM550 cryostat and collected every 20 μm throughout the intracerebroventricular injection site. Sections were stained with antibodies against arginase I (1:200; Santa Cruz Biotechnology) and Iba-1 (1:1000; Wako Chemicals) for fluorescent staining. Images were taken from the region adjacent to the intracerebroventricular injection site and up to 100 μm distal to the injection site for imaging of the choroid plexus.

DRG cultures. DRG neurons were fixed with 2% formaldehyde for 20 min and stained with β-tubulin-III (1:2000; Sigma). Images were taken every 1500 μm across a coverslip with a Carl Zeiss Axioplan 2 Imaging microscope and analyzed using MetaMorph Analysis software (Molecular Devices). Only images that contained a DRG neuronal cell body were analyzed. Neurite growth was determined by the proportional area of β-tubulin-III labeling. DRG cell bodies were excluded in the analysis of β-tubulin-III proportional area.

Statistical analysis. Data were subjected to the Shapiro–Wilk test using Statistical Analysis Systems (SAS) statistical software. To determine significant main effects and interactions between main factors, data were analyzed using one-way (i.e., Pretreatment and Treatment), two-way (i.e., Pretreatment × Treatment), or three-way (i.e. Pretreatment × Treatment × Time) ANOVA using the general linear model procedures of SAS. When appropriate, differences between treatment means were evaluated by an *F*-protected *t* test using the least-significant difference procedure of SAS. In addition, data showing the percentage of mice that

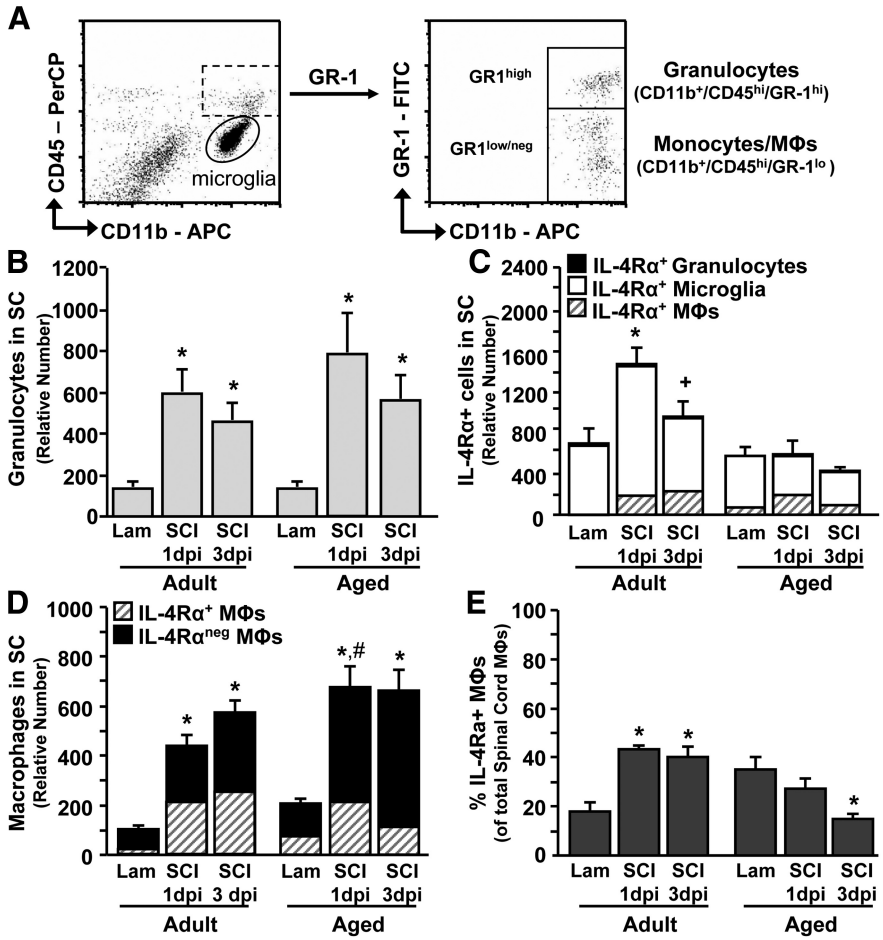

Figure 2. Recruitment of IL-4Rα$^+$ cells to the injured spinal cord was impaired in aged mice. Adult female (3–4 months) and aged female (18–22 months) BALB/c mice were subjected to a T9 laminectomy (Lam) or SCI. After 1 dpi or 3 dpi, enriched CD11b$^+$ cells from the spinal cord were isolated. ***A***, Representative dot plots of CD11b/CD45 and CD11b/GR-1 labeling for microglia (CD11b$^+$/CD45^{lo}) and peripherally derived granulocytes (CD11b$^+$/CD45^{hi}/GR-1^{hi}) and macrophages (CD11b$^+$/CD45^{hi}/GR-1^{lo}). ***B***, Relative number of granulocytes associated with the spinal cord (SC) out of 10,000 live cells ($n = 4–5$). ***C***, Relative number of IL-4Rα$^+$ granulocytes, microglia, and macrophages (MΦs) associated with the spinal cord out of 20,000 live cells ($n = 4–5$). ***D***, Relative number of IL-4Rα$^+$ and IL-4Rα$^-$ macrophages associated with the spinal cord out of 10,000 live cells ($n = 4–5$). ***E***, Percentage of IL-4Rα$^+$ macrophages of the total macrophage population associated with the spinal cord ($n = 4–5$). Error bars represent the mean ± SEM. Means with $^*p < 0.01$ are significantly different and means with $^+p = 0.09$ tend to be different from their Age-matched-Lam control. Means with $^\#p < 0.04$ are significantly different from Adult-SCI-1 dpi.

achieved a particular BMS score or level of arginase expression were evaluated by the χ^2 test. All data are expressed as treatment means ± SEM. Values were considered significant at $p < 0.05$ and a tendency at $p \leq 0.1$.

Results

Age-related impairment in the induction of IL-4Rα surface expression on microglia after SCI

We previously reported that peripheral challenge with LPS, a potent activator of the innate immune system, markedly increased surface expression of IL-4Rα on microglia of adult, but not aged mice (Fenn et al., 2012). Impaired induction of IL-4Rα on microglia from aged mice corresponded with reduced sensitivity to *ex vivo* IL-4 stimulation (Fenn et al., 2012). To test if these age-associated deficits in M2a-mediated regulation would persist *in vivo* after an SCI, adult (3–4 months) and aged (18–19 months) mice were subjected to a moderate (75 kdyn) midthoracic (T9) laminectomy or spinal cord contusion injury (SCI). IL-4Rα protein expression was determined on spinal cord microglia (CD11b$^+$/CD45^{lo}) at 1 dpi or 3 dpi (Fig. 1*A*,*B*). Adult and aged microglia were analyzed using separate age-matched isotype controls because of higher autofluorescence in aged microglia as a result of lipofuscin accumulation (Fig. 1*B*; Xu et al., 2008; Fenn et al., 2012). Fig. 1, *A–C*, shows that a moderate SCI increased microglial surface expression of IL-4Rα in the spinal cord of adult mice at 1 dpi ($p < 0.006$) and 3 dpi ($p = 0.08$), but was not increased on microglia of aged mice at either time point (Age × SCI: $F_{(2,33)} = 10.39$, $p < 0.008$).Thus, SCI-induced IL-4Rα expression on microglia was impaired in aged mice.

Next, two 1 mm sections of the spinal cord adjacent to the injury epicenter were collected for mRNA expression of IL-4 and IL-13. IL-4 mRNA was significantly increased 3 dpi independent of age ($p < 0.02$; Fig. 1*D*). In contrast, IL-13 mRNA was reduced after SCI, but only in adult mice (Age × SCI: $F_{(2,23)} = 6.11$, $p < 0.01$). Although aged mice had lower IL-13 levels at baseline ($p < 0.04$), IL-13 mRNA was maintained after SCI in aged mice and was significantly higher at 3 dpi compared with adult mice ($p < 0.05$). Therefore, microglial IL-4Rα induction was impaired with age, but IL-4 and IL-13 levels were maintained or increased in aged mice after SCI.

Diminished presence of IL-4Rα$^+$ myeloid cells in the spinal cord of aged mice after injury

A hallmark of SCI is the active recruitment of peripheral myeloid cells (i.e., granulocytes, monocytes) to the injury site (Popovich et al., 1997; Sroga et al., 2003; Shechter et al., 2009, 2013). As these cells may also express IL-4Rα, IL-4Rα expression was determined on granulocytes (CD11b$^+$/CD45^{hi}/GR-1^{hi}) and monocytes/macrophages (CD11b$^+$/CD45^{hi}/GR-1^{lo}) in the spinal cord at 1 and 3 dpi. The flow cytometric gating strategy is illustrated in Fig. 2*A*. Both monocytes and macrophages are described here as macrophages. Fig. 2*B* shows that the relative number of GR1^{hi} granulocytes was increased 1 dpi ($p < 0.0001$) and 3 dpi ($p < 0.0001$) independent of age. Moreover, GR-1^{hi} granulocytes did not express high levels of IL-4Rα (Fig. 2*C*). Indeed, >95% of the IL-4Rα$^+$, peripherally derived cells were GR-1^{lo} macrophages (data not shown). Of the IL-4Rα$^+$ myeloid cells after SCI, ~70–75% were microglia and ~25–30% were macrophages (Fig. 2*C*). Fig. 2*C* shows that by combining the contribution of granulocytes, macrophages, and microglia the total relative number of IL-4Rα$^+$ cells was robustly increased in the spinal cord of adult mice at 1 dpi ($p < 0.01$) and 3 dpi ($p = 0.09$), whereas the IL-4Rα$^+$ cell number remained unchanged in aged mice at either time point (Age × SCI: $F_{(2,33)} = 4.83$, $p < 0.02$; Fig. 2*C*).

Next, we investigated if the proportion of macrophages recruited or maintained in the injured spinal cord differed with age. At 1 dpi the total relative number of macrophages (both IL-4Rα$^-$

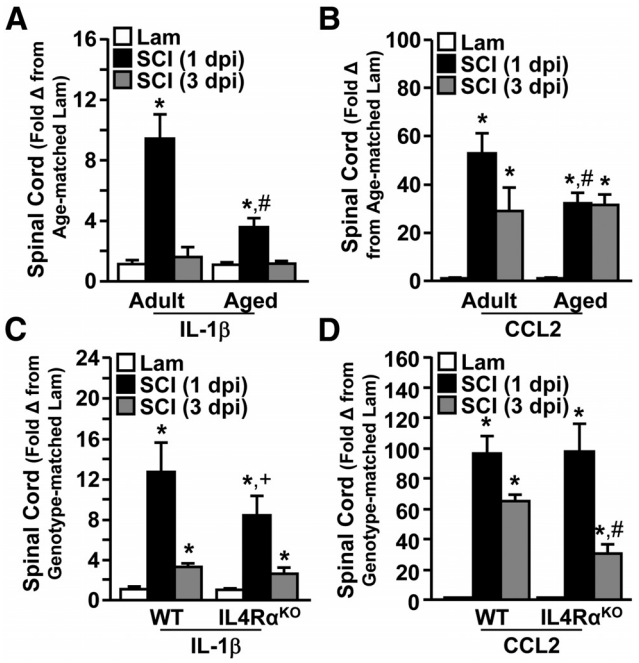

Figure 3. Enhanced IL-1β and CCL2 mRNA expression in adult WT mice after SCI. ***A***, ***B***, Adult female (3–4 months) and aged female (18–22 months) BALB/c mice, and (***C***, ***D***) adult male WT (2–4 months) and adult male (3–4 months) IL-4Rα-deficient (IL-4Rα^{KO}) BALB/c mice were subjected to a T9 laminectomy (Lam) or SCI. Two 1 mm sections of spinal cord were collected adjacent to the epicenter. mRNA expression of (***A***, ***C***) IL-1β and (***B***, ***D***) CCL2 ($n = 4–5$). Error bars represent the mean ± SEM. Means with $^{*}p < 0.05$ are significantly different from Age-matched and genotype-matched-Lam controls. Means with $^{\#}p < 0.0001$ are significantly different and means with $^{+}p = 0.09$ tend to be different from Time point-matched Adult-SCI or WT-SCI groups.

and IL-4Rα^{+}) in the spinal cord of aged mice was increased compared with adult mice ($p < 0.04$; Fig. 2*D*). Despite this increase in macrophage number, the proportion of IL-4Rα^{+} macrophages was reduced in aged mice from ~35% at baseline down to <15% by 3 dpi ($p < 0.01$; Fig. 2*E*) and the proportion of IL-4Rα^{+} macrophages was increased in adult mice from ~18% at baseline, to >40% at 1 and 3 dpi ($p < 0.0002$). Collectively, these data indicate that there is impaired induction of IL-4Rα on microglia of aged mice associated with an altered distribution of IL-4Rα^{+} macrophages after SCI.

Enhanced IL-1β and CCL2 mRNA expression in adult mice after SCI

Because macrophage recruitment after SCI was affected by age, mRNA expression of two key mediators of myeloid cell recruitment (IL-1β and CCL2) were measured proximal to the injury epicenter. In these experiments, adult WT, aged WT, and adult IL-4Rα^{KO} mice were used. All mice for these experiments were on a BALB/c background. Fig. 3*A* shows that IL-1β mRNA was significantly increased at 1 dpi ($p < 0.0001$), but was higher in the spinal cords of adult mice compared with aged mice (Age × SCI: $F_{(1,23)} = 14.95$, $p < 0.001$). Similarly, adult mice had exaggerated expression of CCL2 mRNA 1 dpi compared with aged mice (Age × SCI: $F_{(1,23)} = 6.03$, $p < 0.03$; Fig. 3*B*). By 3 dpi IL-1β and CCL2 mRNA expression levels were not different between age groups. A similar profile of IL-1β and CCL2 mRNA expression was detected in adult IL-4Rα^{KO} mice compared with WT controls. Indeed, IL-1β and CCL2 mRNA expression were reduced in IL-4Rα^{KO} mice compared with WT mice at 1 and 3 dpi, respectively (IL-1β: $p = 0.09$; CCL2: $p < 0.0001$; Fig. 3*C*,*D*). Functional IL-4Rα signaling in adult WT mice corresponded with increased expression of IL-1β and CCL2 and enhanced recruitment of IL-4Rα^{+} macrophages to the injured spinal cord.

Arginase protein expression was reduced in the injured spinal cord of aged mice

Here we show that IL-4Rα induction on microglia was impaired in aged mice after SCI. Our previous studies indicate that a lack of IL-4Rα induction results in reduced IL-4-mediated arginase (Fenn et al., 2012). Therefore, arginase, a key marker of M2a microglia/macrophages, was determined in adult WT, aged WT, and adult IL-4Rα^{KO} BALB/c mice 7 dpi. This time point (7 dpi) represents the peak of arginase expression after SCI in adult mice (Kigerl et al., 2009). Fig. 4, *A* and *B*, shows representative labeling of arginase and TomL in adult WT, aged WT, and adult IL-4Rα^{KO} mice after SCI. Similar to our previous work (Sroga et al., 2003; Kigerl et al., 2009), a dense accumulation of TomL^{+} microglia/macrophages was evident in the injury epicenter. Moreover, arginase protein was increased after SCI and colocalized specifically with TomL^{+} microglia/macrophages (Fig. 4*B*,*C*).

Consistent with impaired IL-4Rα upregulation on microglia/macrophages of aged mice, arginase expression was significantly reduced in the epicenter of Aged-SCI mice ($p < 0.009$) compared with Adult-SCI mice (tendency for SCI × Age: $F_{(1,15)} = 3.40$, $p = 0.09$; Fig. 4*D*). A similar pattern of reduced arginase expression was evident in adult IL-4Rα^{KO} mice compared with WT mice ($p < 0.02$; Fig. 4*D*). These data indicate that IL-4Rα-dependent arginase induction was significantly reduced in myeloid cells of aged mice 7 dpi.

Aged mice had impaired functional recovery and extended lesion length after SCI

Reduced arginase expression in the injured spinal cord of aged mice may point to deficiencies in endogenous repair and worse functional recovery after SCI. To test this, functional recovery was assessed over a 28 d period after SCI using the BMS (Basso et al., 2006; Fig. 5*A*). Age alone did not influence the BMS score for uninjured mice as all Lam controls had similar scores over the 28 d testing period. Following SCI, however, both adult and aged BALB/c mice exhibited significant motor impairments that improved over the 28 d time period (SCI × Time: $F_{(6,153)} = 19.57$, $p < 0.0001$). Nonetheless, spontaneous recovery was significantly reduced in aged mice compared with adult mice at 1, 3, 5, 7, 21, and 28 dpi (Age × SCI: $F_{(1,153)} = 12.96$, $p < 0.0001$).

A significant functional milestone in recovery from SCI is the ability to achieve frequent or consistent bilateral weight-supported stepping. Mice that achieved a BMS score of 5 have achieved this recovery milestone. Fig. 5*B* shows that ~75% of the Adult-SCI mice achieved a BMS score of 5 by 28 dpi, but none of the Aged-SCI mice reached this level of recovery ($p < 0.0001$). Aged mice averaged a BMS score of 3 associated with hindlimb plantar placement, but without stepping.

After the completion of locomotor testing at 28 dpi, the percentage of tissue sparing and total lesion length was determined (Donnelly et al., 2011). Although tissue sparing at the lesion epicenter was reduced by 10% in aged spinal cords, this was not significantly different from adults (Fig. 5*C*). Lesion length, however, was 38% longer in Aged-SCI mice compared with Adult-SCI mice ($p = 0.06$; Fig. 5*D*,*E*). Indeed, 1.2 mm rostral and caudal of the epicenter Aged-SCI tissue still showed evidence of a lesion, whereas the lesion was not present in Adult-SCI mice at this distance (Fig. 5*D*). Thus, aged mice had reduced functional

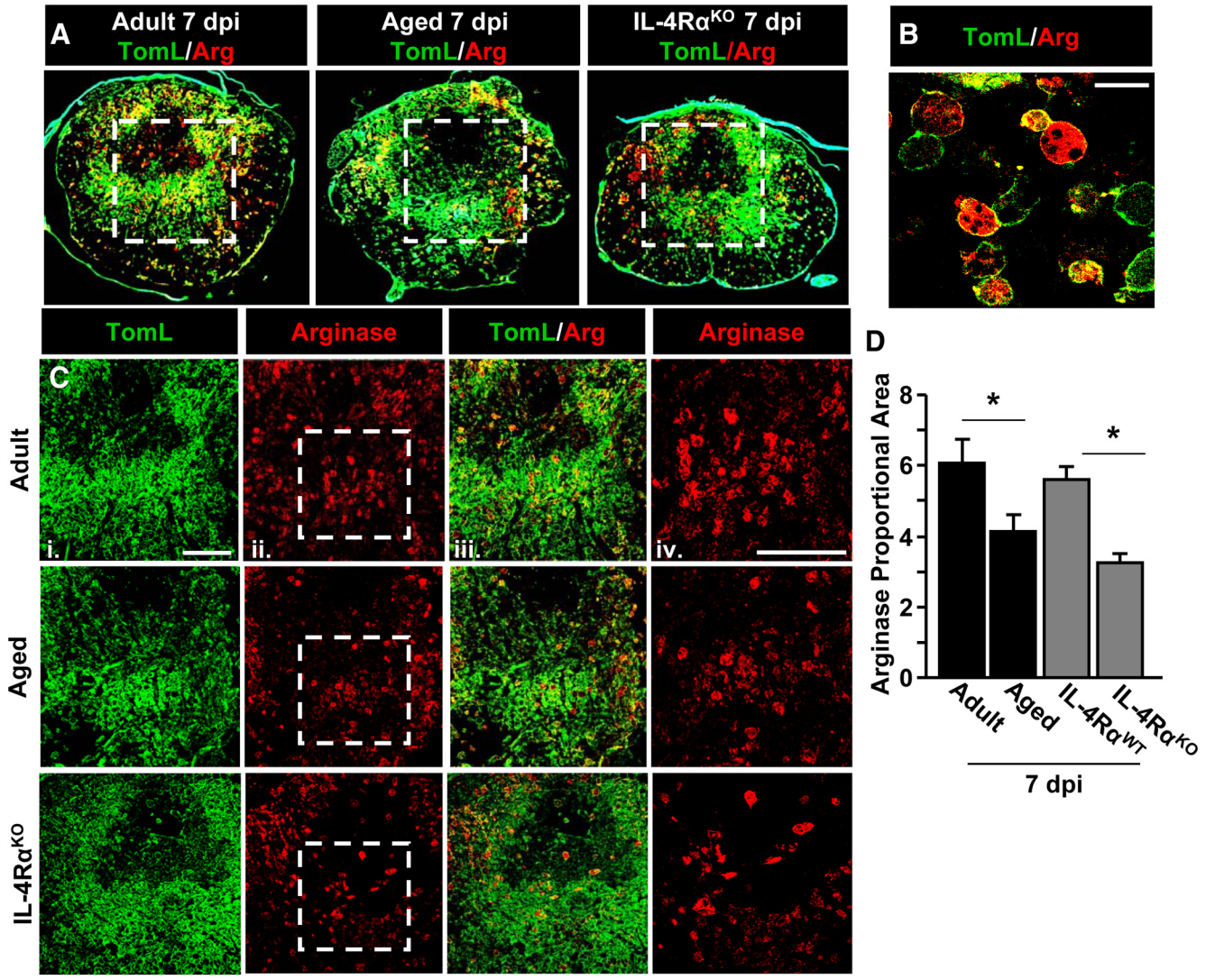

Figure 4. Arginase protein expression was reduced in the injured spinal cord of aged and IL-4Rα^{KO} mice. Adult female (3–4 months), aged female (18–22 months), adult male WT (2–4 months), and adult male IL-4Rα^{KO} (3–4 months) BALB/c mice were subjected to a T9 laminectomy (Lam) or SCI. Spinal cords were collected 7 dpi. ***A***, Representative images of the injury epicenter in adult, aged, and adult IL-4Rα^{KO} mice labeled with TomL (green) and arginase (Arg; red). Dashed white box shows the area represented in ***C*** used for quantitative analysis. ***B***, Representative image of TomL/Arg labeling in the epicenter at 63× magnification. Scale bar, 25 μm. ***C***, Representative images of TomL (***i***), Arg (***ii***), and TomL/Arg (***iii***) labeling. Dashed white box shows the area represented in ***iv*** at 40× magnification. Scale bar, 200 μm. ***D***, Quantification of Arg staining in adult, aged, adult WT, and adult IL-4Rα^{KO} mice ($n = 4–6$). Error bars represent the mean ± SEM. Means with $^*p < 0.01$ are significantly different from Adult or WT controls.

recovery and an extended lesion size compared with adult mice following SCI.

To evaluate the extent to which reduced IL-4Rα expression contributed to functional recovery deficits in aged BALB/c mice, functional recovery was tested in WT and IL-4Rα^{KO} BALB/c mice 28 d after SCI. Similar to aged mice, adult IL-4Rα^{KO}-SCI mice showed worse functional recovery at 28 dpi compared with adult WT-SCI mice. For example, similar to other immune receptor KOs (e.g., TLR2^{KO}; Kigerl et al., 2007), IL-4Rα^{KO} mice did not significantly differ in BMS score compared with WT mice (data not shown) but had a BMS subscore that was ~73% lower than WT controls ($p = 0.07$; Fig. 5*F*). Moreover, 50% of WT mice achieved a BMS score of 5, whereas only 33% of IL-4Rα^{KO} mice achieved this functional milestone (Fig. 5*G*). Also, 25% of WT mice achieved a BMS score of 6 (frequent/consistent stepping with some coordination) but 0% of IL-4Rα^{KO} mice reached this score (Fig. 5*H*). Collectively, these studies indicate that reduced IL-4Rα expression in IL-4Rα^{KO} and aged mice contributes to impaired functional recovery after SCI.

IL-4Rα induction on activated microglia was required for IL-4-dependent arginase expression

Our data indicate that aged mice had reduced functional recovery after SCI associated with impaired microglial induction of IL-4Rα. An age-related deficit in IL-4Rα upregulation corresponded with attenuated arginase expression, reduced IL-1β and CCL2 expression, and reduced presence of IL-4Rα$^+$ macrophages in the injured spinal cord. Nonetheless, it is difficult to understand the significance of enhanced or impaired IL-4/IL-4Rα signaling in microglia after SCI because the onset and nature of the inflammatory stimulus is not known, arginase induction is partially IL-4-indpendent (Fig. 4*C*), and various cross-signaling mechanisms likely control the magnitude and effect of inflammation. Therefore, we moved to an immune-based model in adult mice in which the inflammatory stimulus (LPS) and delivery of IL-4 could be better controlled and M2a profile examined.

Adult BALB/c mice were surgically implanted with an indwelling cannula in the lateral ventricle. After 7 d, mice were

given an intraperitoneal injection of saline or LPS to promote an inflammatory response in the CNS. After 1 h, mice were then given an intracerebroventricular injection of vehicle or IL-4. Fig. 6*A* shows that 24 h after LPS, IL-4Rα expression was upregulated on microglia in the spinal cord ($p < 0.05$) and the brain ($p < 0.05$) to a similar extent. Because cannulas for central IL-4 infusion can be better established in the brain, we investigated IL-4/IL-4Rα-induced M2a responses in brain-resident microglia. Fig. 6*B* shows that intracerebroventricular administration of IL-4 increased mRNA expression of arginase by ~10-fold, and this induction was augmented over 160-fold in mice that were pretreated with LPS (LPS × IL-4: $F_{(1,32)} = 4.4$, $p < 0.05$). Peripheral injection of LPS alone, however, did not increase arginase mRNA expression.

To confirm these mRNA results and to determine the extent to which the induction of arginase was microglia specific, arginase protein was measured in brain-resident microglia (Iba-1$^+$) proximal to the intracerebroventricular injection site (Fig. 6*C*). Representative images of Iba-1 (Fig.6*Di*, green) and arginase (Fig.6*Dii*, red) labeling are shown. Arginase protein was not present in the brain of the control mice (Saline-Vehicle) or mice injected with just LPS (LPS-Vehicle; Fig. 6*D*,*F*). Although a low level of arginase was induced by IL-4 (Saline-IL-4) consistent with the mRNA data (Fig. 6*B*), this was not significantly different from control mice. Arginase protein, however, was markedly increased in the brain of mice that received both peripheral LPS and intracerebroventricular IL-4 (LPS × IL-4: $F_{(1,14)} = 23.72$, $p < 0.0005$; Fig. 6*D*,*F*). Moreover, this robust induction of arginase was detected specifically in Iba-1$^+$ microglia (Fig. 6*Div*,*E*). These data indicate that inflammatory-induced IL-4Rα upregulation on microglia is required for these cells to respond to IL-4 and increase arginase protein expression.

After SCI, aged mice had deficits in microglial IL-4Rα induction with corresponding impairments in arginase protein expression. Therefore, the same immune-based protocol as above was also performed in a subset of adult (3 months) and aged (20 months) BALB/c mice to assess arginase protein expression. Representative images of the Adult-LPS-IL-4 group and Aged-LPS-IL-4 group are shown (Fig. 6*G*). Increased lipofuscin accumulation in the brain with age often results in increased background labeling for immunohistochemistry or flow cytometry (Sierra et al., 2007; Xu et al., 2008; Fenn et al., 2012). Indeed, arginase labeling was sevenfold higher in Aged-Saline-Vehicle controls compared with adult-Saline-Vehicle controls (data not shown). Thus, to assess the level of exaggerated arginase expression in the Aged-LPS-IL-4 group, arginase protein expression was compared with age-matched Saline-IL-4 controls. Fig. 6*H* shows that IL-4-mediated reprogramming of active microglia to an arginase$^+$ phenotype was attenuated by 79% in the brain of aged mice compared with adults. These data indicate that reprogramming of activated microglia by IL-4 was impaired with age. Thus, a robust induction of arginase *in vivo* required (1) an inflammatory/activating signal and (2) responsiveness to an M2a reprogramming signal.

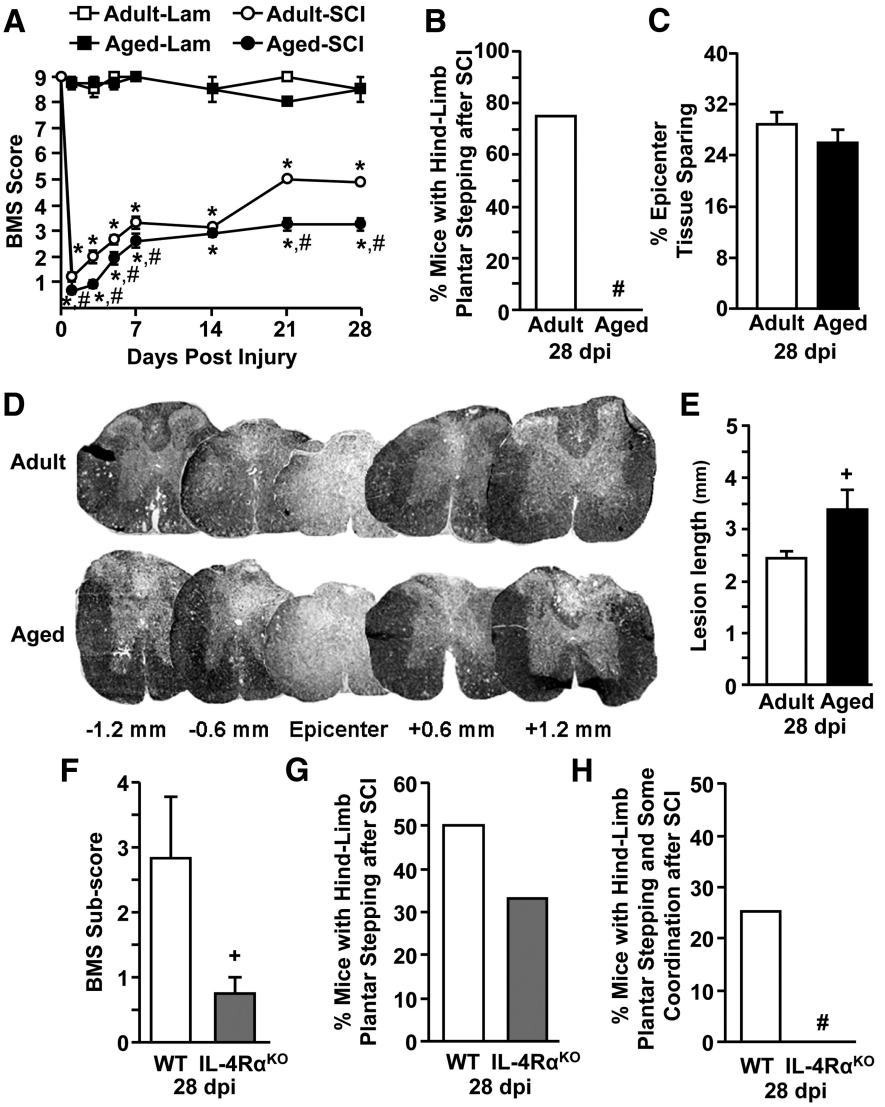

Figure 5. Aged mice had impaired functional recovery and extended lesion length after SCI. Adult female (3–4 months) and aged female (18–22 months) BALB/c mice were subjected to a T9 laminectomy (Lam) or SCI. Functional recovery was assessed by BMS scoring over a 28 d period after SCI. Spinal cords were collected 28 dpi. ***A***, BMS scores for 1, 3, 5, 7, 14, 21, and 28 dpi for Lam controls ($n = 4$) and SCI mice ($n = 10–13$). ***B***, Percentage of adult and aged SCI mice that achieved an average BMS score of ≥5 at 28 dpi. ***C***, Quantification of epicenter tissue sparing using neurofilament/EC staining ($n = 4$). ***D***, Representative images of neurofilament/EC staining in injured spinal cord of adult and aged mice 1.2 mm rostral and caudal of the epicenter. Dark staining denotes intact axons and myelin sheathing. ***E***, Lesion length from adult and aged mice ($n = 4$). In a separate study, adult male WT (2–4 months) and adult male IL-4Rα^{KO} (3–4 months) BALB/c mice were subjected to a T9 Lam or SCI. ***F***, BMS subscore for WT and IL-4Rα^{KO} mice at 28 dpi ($n = 8$). ***G***, Percentage of WT and IL-4Rα^{KO} SCI mice that achieved an average BMS score of 5 at 28 dpi ($n = 8$). ***H***, Percentage of WT and IL-4Rα^{KO} SCI mice that achieved an average BMS score of 6 at 28 dpi ($n = 8$). Error bars and data points represent the mean ± SEM. Means with $^*p < 0.0001$ are significantly different from Adult-Lam controls. Means with $^\#p < 0.03$ are significantly different from Adult-SCI or WT-SCI groups. Means with $^+p = 0.07$ tend to be different from Adult-SCI or WT-SCI groups.

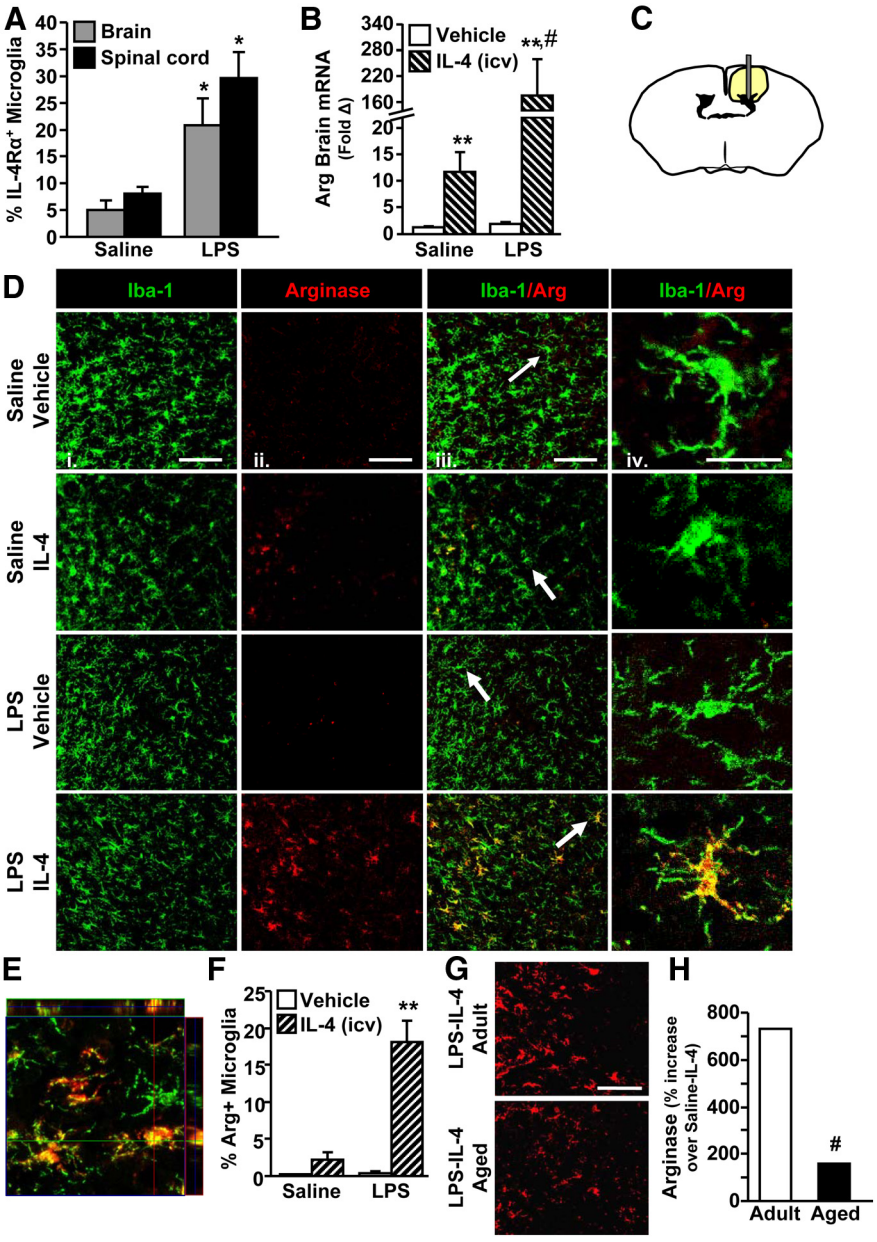

Figure 6. IL-4Rα induction on activated microglia was required for IL-4-dependent arginase expression. Adult (3 months) male BALB/c mice received an intraperitoneal injection of saline or LPS and 1 h later received an intracerebroventricular (icv) injection of vehicle or IL-4. Brains and spinal cords were collected 24 h after LPS. ***A***, Enriched microglia were isolated from the brain and enriched CD11b$^+$ cells were isolated from the spinal cord. Average percentage of IL-4Rα$^+$ microglia by flow cytometry (n = 2–3). ***B***, mRNA expression of arginase (Arg) from a 1 mm coronal section at the intracerebroventricular injection site (n = 8–18). ***C***, Schematic of the area where images were collected for Iba-1/Arg labeling. ***D***, Representative images of Iba-1 (***i***), Arg (***ii***), and Iba-1/arginase (***iii***) labeling. Scale bars, 100 μm. White arrows indicate microglia used for higher magnification in ***iv***. Scale bar, 25 μm. ***E***, Representative image for orthogonal analysis of colocalization for Iba-1 (green)/Arg (red) labeling. ***F***, Percentage Iba-1$^+$/Arg$^+$ microglia (n = 3–4). ***G***, A separate subset of adult (3 months) and aged (20 months) male BALB/c mice were given Sal/LPS and Vehicle/IL-4 injections as above. Brains were collected 24 h after LPS. Representative images for Arg staining. Scale bar, 50 μm. ***H***, Percentage increase in Arg staining for LPS-IL-4 mice compared with age-matched Saline-IL-4 controls (n = 3). Error bars represent the mean ± SEM. Means with *$p < 0.05$ are significantly different from Saline controls. Means with **$p < 0.01$ are significantly different from Saline-Vehicle controls. Means with $^{\#}p < 0.01$ are significantly different from Adult-Saline-IL-4.

IL-4-mediated reprogramming of activated microglia supported neurite outgrowth

Previous studies show that M2a microglia/macrophages (arginase$^+$) promote axon growth *in vitro* and enhance remyelination *in vivo* (Kigerl et al., 2009). Whether or not a similar repair potential is elicited in microglia primed by an inflammatory stimulus has not been tested. Therefore, axon growth was determined in adult DRG neurons cocultured with inflammatory-activated microglia, with or without IL-4. Adult BALB/c mice were injected intraperitoneally with saline or LPS. After 4 h microglia were isolated and cultured *ex vivo* in transwell inserts placed directly over DRG neurons isolated from adult BALB/c mice 3 d prior. Cocultures were then treated with either vehicle or IL-4 and neurite outgrowth was measured 24 h later. Fig. 7*A* shows representative images from the four different experimental groups. There was a significant interaction between microglia activation and IL-4 stimulation (LPS × IL-4, $F_{(1,20)} = 4.77$, $p < 0.05$) on DRG axon outgrowth (e.g., increased proportional area of β-tubulin-III staining). For instance, β-tubulin-III proportional area was reduced when neurons were cocultured with inactive microglia treated with IL-4 (Sal-IL-4; $p < 0.03$). Moreover, β-tubulin-III proportional area was unaffected by coculture with active microglia alone (LPS-Vehicle). β-tubulin-III proportional area was highest, however, when DRG neurons were cocultured with active microglia reprogrammed with IL-4 (LPS-IL-4; $p = 0.1$; Fig. 7*B*). These data are interpreted to indicate that IL-4-mediated reprogramming of activated microglia supported neurite outgrowth and complexity.

IL-4-mediated reprogramming of activated microglia augmented mRNA expression of IL-1β and CCL2

Differential distribution of macrophages in the aged spinal cord after SCI was associated with impaired IL-4Rα induction on microglia, reduced arginase expression, and reduced mRNA expression of IL-1β and CCL2. The LPS model confirmed that IL-4-mediated reprogramming of inflammatory microglia induced a robust arginase response similar to that observed after Adult-SCI. Therefore, IL-1β and CCL2 mRNA were measured in a coronal brain section 24 h after LPS and IL-4 treatments in adult BALB/c mice. As expected, microglial mRNA expression of IL-1β was increased 24 h after LPS compared with saline controls ($p = 0.08$; Fig. 8*A*). Consistent with the SCI studies, IL-1β mRNA expression was further enhanced by intracerebroventricular IL-4 treatment (LPS × IL-4, $F_{(1,44)} = 5.40$, $p < 0.03$). A similar pattern was evident for brain CCL2 in that injection with peripheral LPS and intracerebroventricular IL-4 resulted in enhanced mRNA expression compared with LPS alone (LPS × IL-4: $F_{(1,35)} = 11.17$, $p < 0.003$; Fig. 8*B*).Together, post treatment with IL-4 *in vivo* enhanced expression of

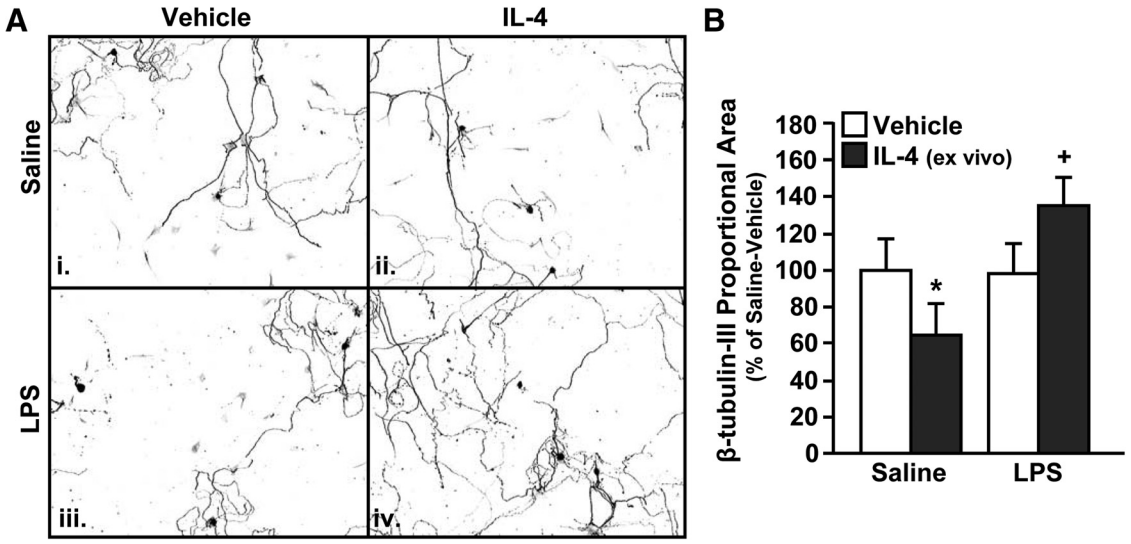

Figure 7. IL-4-mediated reprogramming of activated microglia supported neurite outgrowth *ex vivo*. Adult (3 months) male BALB/c mice received an intraperitoneal injection of saline or LPS and 4 h later enriched microglia were isolated. Enriched microglia were plated in transwell inserts directly over DRG neurons collected from adult (3 months) male BALB/c mice. Cultures were treated with vehicle or IL-4 for 24 h. ***A***, Representative images of β-tubulin-III staining of DRG neurons. ***B***, β-tubulin-III proportional area as a percentage of Saline-Vehicle ($n = 6–8$). Error bars represent the mean ± SEM. Means with $^{*}p < 0.03$ are significantly different and means with $^{+}p = 0.1$ tend to be different from Saline-Vehicle controls.

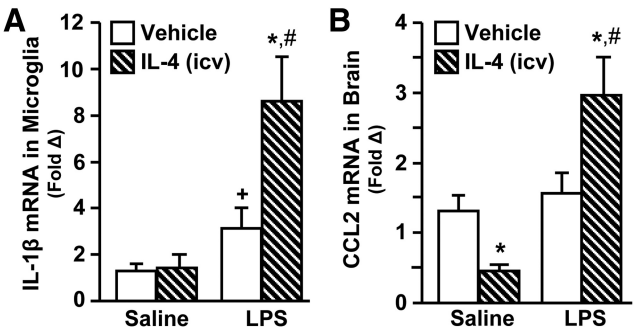

Figure 8. IL-4-mediated reprogramming of activated microglia augmented mRNA expression of IL-1β and CCL2. Adult (3 months) male BALB/c mice were given an intraperitoneal injection of saline or LPS and 1 h later received an intracerebroventricular (icv) injection of vehicle or IL-4. Brains were collected 24 h after LPS. A 1 mm coronal brain section was taken and the remainder of the brain was used to isolate enriched microglia. ***A***, mRNA expression of IL-1β in enriched microglia ($n = 8–14$). ***B***, mRNA expression of CCL2 from a coronal brain section ($n = 7–11$). Error bars represent the mean ± SEM. Means with $^{*}p < 0.05$ are significantly different and means with $^{+}p = 0.1$ tend to be different from Saline-Vehicle controls. Means with $^{\#}p < 0.04$ are significantly different from LPS-Vehicle.

inflammatory-associated factors IL-1β and CCL2 compared with treatment with LPS alone.

IL-4-mediated reprogramming of activated microglia increased the trafficking of CCR2^{+} macrophages to the brain

We show increased mRNA expression of IL-1β and CCL2 at 1 dpi in the spinal cord of adult mice compared with aged mice (Fig. 3) and that IL-4 reprogramming of active microglia promoted the expression of IL-1β and CCL2 (Fig. 8). This is important because these are two critical factors associated with recruitment of macrophages to the CNS. Indeed, increased IL-1β and CCL2 corresponded with increased association of IL-4Rα^{+} macrophages with the spinal cord of adult mice (Fig. 2). Therefore, we sought to determine the extent to which IL-4 promotes macrophage recruitment to the CNS in our immune-based studies. To assess macrophage trafficking C57BL/6 mice were used (Wohleb et al., 2013). First, IL-4Rα induction on enriched microglia of WT C57BL/6 mice after LPS was confirmed, and this induction was unaffected by intracerebroventricular IL-4 (data not shown). Second, the relative proportion of microglia and brain-associated macrophages was determined after intraperitoneal LPS and intracerebroventricular IL-4 injections. Representative bivariate dot plots of CD11b and CD45 labeling on Percoll-isolated brain microglia (CD11b^{+}/CD45^{lo}) and macrophages (CD11b^{+}/CD45^{hi}) are shown (Fig. 9*A*). Consistent with the SCI studies, Fig. 9*B* shows that the highest percentage of brain-associated macrophages was measured in mice with activated microglia reprogrammed by intracerebroventricular IL-4 (LPS-IL-4, $p < 0.04$). Next, the phenotype of recruited macrophages was investigated. IL-4Rα expression was assessed on macrophages following a saline or LPS injection alone. In these experiments 65% of IL-4Rα^{+} cells were also CCR2^{+} (data not shown). Of the CCR2^{+} macrophages, only 5% expressed IL-4Rα protein under basal conditions (Saline) and this proportion increased to >20% after LPS injection (Fig. 9*C*). Thus, IL-4Rα is expressed primarily on CCR2^{+} macrophages and CCR2^{+} macrophages increase their expression of IL-4Rα following an LPS challenge.

Next we investigated the recruitment of CCR2^{+} macrophages after intracerebroventricular IL-4 treatment. Fig. 9*D* shows that post treatment with intracerebroventricular IL-4 after LPS enhanced trafficking of CCR2^{+} macrophages to the brain ($p < 0.03$). The expression of CCR2 on a per cell basis (i.e., CCR2 MFI) was also enhanced following LPS-IL-4 treatments compared with LPS-Veh controls (Fig. 9*E*, $p = 0.1$). Analysis of both CCR2 and CX_3CR1 expression on brain-associated macrophages indicated that CCR2^{+} cells were selectively retained or recruited after LPS and IL-4 (77 ± 3%) compared with LPS alone (66 ± 3%, $p < 0.05$; Fig. 9*E*). The breakdown of the expression of CCR2 and CX_3CR1 is shown in the LPS-Veh and LPS-IL-4 groups in Fig. 9*E*. Compared with LPS alone (LPS-Veh), there was a relative increase in the percentage of CCR2^{+}/CX_3CR1^{lo} (67% from 60%) and CCR2^{+}/CX_3CR1^{neg} macrophages (10% from 3%), and relative reduction in the percentage of CCR2^{neg}/CX_3CR1^{hi} (19% from 27%) and CCR2^{neg}/CX_3CR1^{neg} (4% from 7%) macrophages in the LPS-IL-4 group.

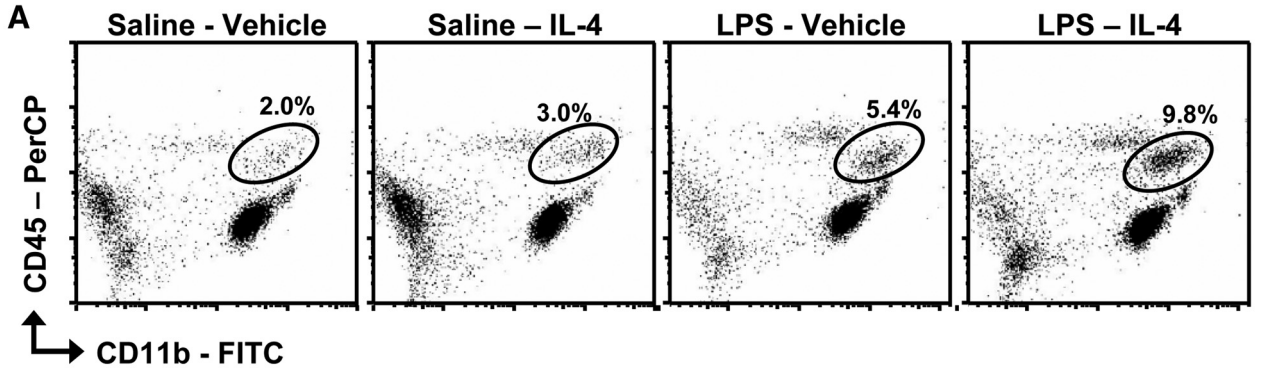

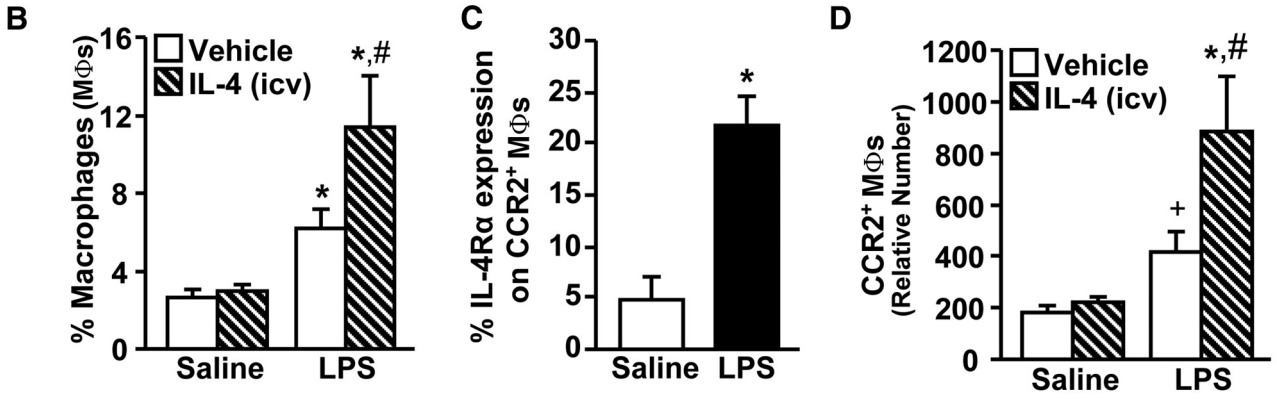

E

CD11b^{+} CD45^{hi}	CCR2 (MFI)	CCR2+	*CCR2+ CX_3CR1^{lo}*	*CCR2+ CX_3CR1^{neg}*	*$CCR2^{neg}$ CX_3CR1^{hi}*	*$CCR2^{neg}$ CX_3CR1^{neg}*
LPS-Veh	118 ± 10.3	66.5 ± 3.4%	60 ± 6.2%	3.0 ± 2.2%	27 ± 2.6%	7 ± 2.4%
LPS-IL-4	158 ± 22.1‡	77.0 ± 3.1%#	67 ± 3.4%	10.0 ± 4.4%	19 ± 3.2%	4 ± 0.5%

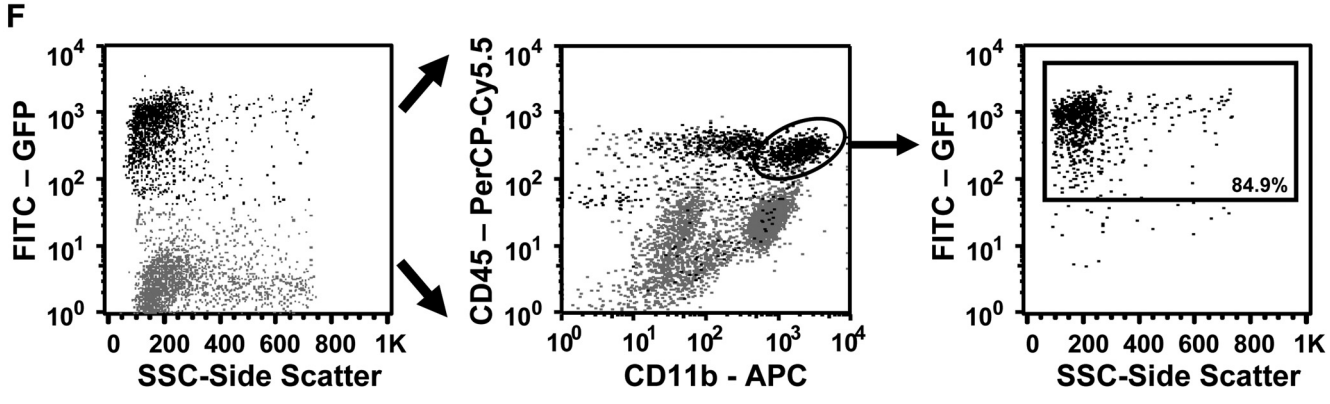

Figure 9. IL-4-mediated reprogramming of activated microglia increased the recruitment of CCR2^{+} macrophages to the brain. Adult (3 months) male C57BL/6 mice were given an intraperitoneal injection of saline or LPS and 1 h later received an intracerebroventricular (icv) injection of vehicle or IL-4. Enriched microglia were isolated from the brain 24 h after LPS. ***A***, Representative dot plots for CD11b/CD45 staining. Oval indicates peripherally derived macrophages (CD11b^{+}/CD45^{hi}). ***B***, Percentage of CD11b^{+}/CD45^{hi} macrophages (MΦs) associated with the brain ($n = 4$–7). ***C***, Percentage of CCR2^{+} macrophages that were IL-4Rα^{+} following Saline or LPS treatment alone ($n = 3$). ***D***, Relative number of CCR2^{+} macrophages associated with the brain out of 10,000 live cells ($n = 4$–7). ***E***, Proportion of CCR2^{+} macrophages and CCR2 MFI in macrophages of LPS-Veh and LPS-IL-4 groups. A breakdown of the proportion of CCR2$^{+/-}$ and $CX_3CR1^{+/-}$ macrophages in LPS-Veh and LPS-IL-4 groups is also shown. ***F***, Partial GFP BM-chimera mice were established on the C57BL/6 background. Mice achieved an average of 60 – 80% engraftment. After 4 weeks mice were injected with intraperitoneal LPS. Representative series of dot plots showing that >80% of the CD11b^{+}/CD45^{hi} cells identified in ***A*** and used for flow analyses were GFP^{+} indicating they derived from a peripheral source. Error bars represent the mean ± SEM. Means with $^{*}p <$ 0.04 are significantly different and means with $^{+}p = 0.07$ tend to be different from Saline-Vehicle controls. Means with $^{\#}p < 0.05$ are significantly different and means with $^{\ddagger}p = 0.1$ tend to be different from LPS-Vehicle.

To confirm that these macrophages were BM derived and to determine their neuroanatomical distribution, GFP BM-chimera mice on a C57BL/6 background were established (Wohleb et al., 2013). Flow cytometric analysis confirmed that the increased population of CD11b$^+$/CD45^{hi} cells 24 h after LPS was peripherally derived (Fig. 9*F*). Next, the neuroanatomical distribution and M2a phenotype (arginase$^+$) was examined at the intracerebroventricular injection site and nearby choroid plexus. Fig. 10*A* shows representative images of GFP$^+$/Iba-1$^+$/arginase$^+$ cells in the injection site 24 h after LPS in LPS-Vehicle and LPS-IL-4 treatment groups. Histological analysis confirmed the flow cytometric studies and revealed that trafficking of BM-derived cells to the brain was significantly increased in LPS-IL-4-treated mice compared with all other groups ($p < 0.03$; Fig. 10*B*). Moreover, these peripherally derived GFP$^+$ cells, similar to resident microglia, were capable of expressing arginase in response to IL-4. Indeed, in mice injected with both intraperitoneal LPS and intracerebroventricular IL-4, ~25% of all GFP$^+$ cells were also arginase$^+$ (Fig. 10*A*). Of the arginase$^+$ cells, ~45% were microglia (Iba-1$^+$), ~40% were peripherally derived cells that had trafficked into the brain parenchyma (GFP$^+$/Iba-1$^+$), and ~15% were peripherally derived cells in the perivascular spaces (GFP$^+$; Fig. 10*C*).Together, IL-4-IL-4Rα-dependent alternative activation of microglia was associated with increased recruitment of BM-derived myeloid cells to the CNS, which in turn, were directed to an arginase$^+$ phenotype.

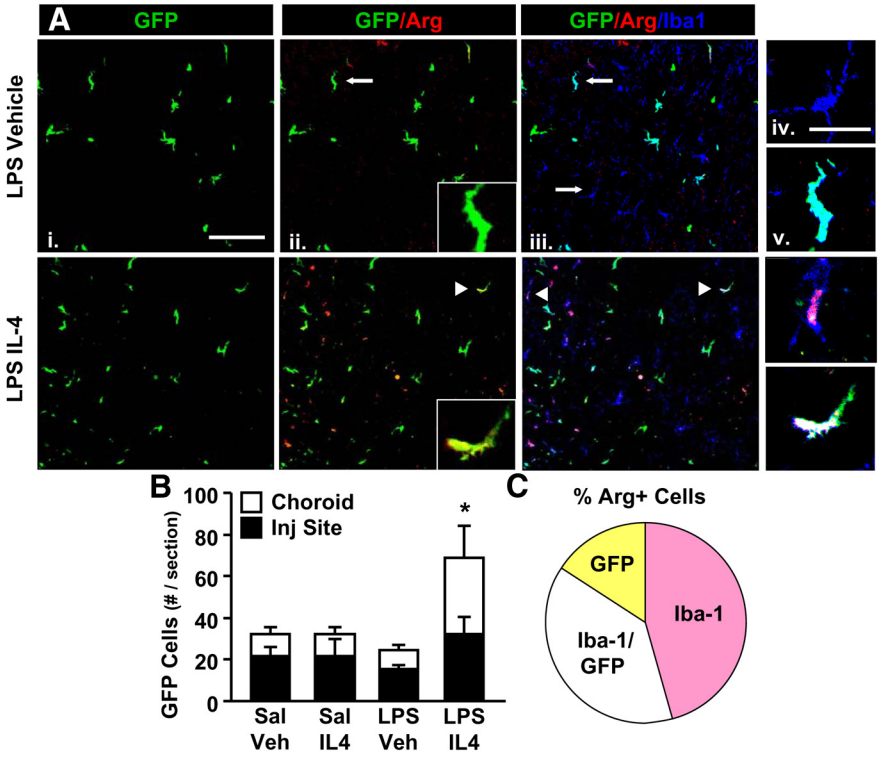

Figure 10. GFP$^+$ macrophages could switch to an arginase$^+$ phenotype after LPS-IL-4 treatment. Partial GFP BM-chimera mice were established on the C57BL/6 background and achieved an average of 60–80% engraftment. After 4 weeks adult (3 months) GFP BM-chimera mice were given an intraperitoneal injection of saline or LPS and 1 h later received an intracerebroventricular (icv) injection of vehicle or IL-4. Mice were perfused and fixed 24 h later. ***A***, Representative images showing GFP (***i***), GFP/Arg (***ii***), and GFP/Arg/Iba-1 (***iii***) staining. Scale bars, 100 μm. White arrows indicate GFP$^+$ or GFP$^+$/Iba-1$^+$ cells used for insets in ***ii***, ***iv***, and ***v***, and white arrowheads indicate Arg$^+$ colocalization with GFP$^+$, Iba-1$^+$, or GFP$^+$/Iba1$^+$ cells used for insets in ***ii***, ***iv***, and ***v***. Scale bars, 25 μm. ***B***, Number of GFP$^+$ cells per section at the icv injection site and nearby choroid plexus ($n = 4–5$). ***C***, Percentage Arg$^+$ cells that were GFP$^+$, Iba-1$^+$, and GFP/Iba-1$^+$ in the LPS-IL-4 group. Error bars represent the mean ± SEM. Means with $^*p < 0.04$ are significantly different from Saline-Vehicle controls.

Discussion

There is significant interest in understanding activation profiles of microglia and macrophages in aging, disease, and CNS injury. Our previous work indicates that IL-4Rα was markedly enhanced on microglia of adult, but not aged mice after a peripheral LPS challenge (Fenn et al., 2012). Moreover, LPS-activated microglia from adult mice were more responsive to IL-4 *ex vivo* than aged mice (Fenn et al., 2012). The primary aim of this study was to determine whether impaired IL-4/M2a microglial regulation in the aged CNS resulted in immune and functional deficits after SCI. The secondary aim was to better understand the role of M2a microglia/macrophages *in vivo* in the context of inflammation and aging. We show original data that IL-4Rα was enhanced after SCI on microglia of adult, but not aged, mice. IL-4Rα upregulation corresponded with increased IL-1β and CCL2 mRNA expression, enhanced association of IL-4Rα$^+$ macrophages with the injured spinal cord, increased arginase expression, and improved functional recovery. Immune-based studies revealed that IL-4-dependent arginase required inflammatory-induced IL-4Rα expression. Moreover, treatment with IL-4 in the inflammatory CNS directly augmented the expression of inflammatory mediators (IL-1β, CCL2) and enhanced CCR2$^+$/IL-4Rα$^+$ macrophage recruitment. Thus, IL-4 drove a unique M2a microglial phenotype (arginase$^+$/IL-1β$^+$), which supported both intrinsic repair and the recruitment of peripheral myeloid cells. Moreover, this phenotype was reduced in aged mice corresponding with limited recovery after SCI.

One important aspect of this study was that aged mice had worse functional recovery after SCI compared with adults. For example, ~75% of adults had frequent or consistent stepping with no coordination (BMS score = 5) by 28 dpi compared with 0% of aged mice that achieved this score. Consistent with a worse BMS score, lesion length was longer in aged mice at 28 dpi. These data are consistent with previous studies showing increased pathology and demyelination (Siegenthaler et al., 2008) and worse functional recovery (Gwak et al., 2004) in middle-aged (12 months) rats after a spinal cord contusion or hemisection. Here we extend these findings in mice of advanced age (18–19 months) and provide evidence of impaired reprogramming of microglia. These data are clinically relevant because no basic models of SCI in advanced ages had been established and a mechanism for worse recovery had not been proposed (Chen et al., 1997; Fassett et al., 2007; National SCI Statistical Center, 2013). Impaired functional recovery at 28 dpi was also recapitulated in adult IL-4Rα^{KO} mice. Together, our data using both models indicate that IL-4/IL-4Rα dysfunction is a key contributing factor to poorer functional recovery after SCI.

A potential mechanism for increased morbidity after SCI in the aged mice is reduced responsiveness to IL-4 by microglia/macrophages. We focused on IL-4 rather than IL-13 because IL-4

was increased in both adult and aged mice after SCI, whereas IL-13 was reduced acutely after SCI in adults. Although the increase in IL-4 mRNA was undetectable until 3 dpi, other studies have detected IL-4 protein from microglia at 1 dpi (Guerrero et al., 2012) corresponding to the time point of IL-4Rα upregulation. The source of IL-4 was not determined here because of a lack of cell specificity in our RNA analyses of the spinal cord, but other studies suggest that IL-4 may derive from spinal cord-resident microglia (Guerrero et al., 2012), or infiltrating myeloperoxidase-positive neutrophils (Lee et al., 2010). Whatever the source, IL-4 mRNA induction in adult and aged mice was the same. Therefore, reduced IL-4Rα, rather than reduced IL-4, was responsible for the less arginase$^+$ myeloid cells in aged mice. These findings are consistent with a previous study showing that equivalent levels of IL-4/IL-13 resulted in attenuated upregulation of IL-4/IL-13-response genes in aged mice compared with adults (Lee et al., 2013). The link between IL-4Rα impairments and reduced arginase, IL-1β, and CCL2 expression in aged mice after SCI was further confirmed using adult IL-4Rα^{KO} mice. Notably, although arginase expression was reduced in the spinal cords of IL-4Rα^{KO} and aged mice, it was not ablated. The role of this IL-4Rα-independent arginase expression remains to be elucidated, but here we demonstrate that reduced IL-4/IL-4Rα-dependent arginase corresponded with an impaired immune response and reduced functional recovery.

Another important aspect of this study was our M2a profile analysis *in vivo* in the context of active inflammation. IL-4-driven M2a responses in microglia/macrophages are primarily reported using *in vitro* culture systems with either pretreatment or cotreatment of IL-4 followed by an inflammatory stimulus. In those studies, IL-4 increased arginase expression and reduced inflammatory mediators including IL-1β and TNF-α (Kitamura et al., 2000; Butovsky et al., 2006; Lyons et al., 2007). *In vivo*, however, IL-4 concentrations are low/undetectable at baseline and are increased after the establishment of an inflammatory response to injury. Thus we aimed to better model these conditions with an immune-based approach in which microglia were activated using a peripheral LPS injection and then IL-4 was provided centrally 1 h later. In both the SCI and LPS-intracerebroventricular IL-4 experiments, IL-4/IL-4Rα-mediated responses increased arginase, but also augmented the expression of IL-1β, and CCL2 in microglia or brain/spinal cord. Thus, this arginase$^+$/IL-1β$^+$ microglia phenotype may better represent an "alternative activation" state *in vivo*. Although this phenotype may be perceived as "inflammatory," it is still beneficial for restricting pathology. For example, intact IL-4/IL-4Rα signaling in Adult-SCI mice corresponded to reduced tissue lesion length and better functional recovery than aged mice. Moreover, the arginase$^+$/IL-1β$^+$ microglial phenotype induced by LPS-IL-4 treatment promoted DRG neurite growth/complexity *ex vivo*. In contrast, IL-4 alone failed to increase arginase protein and DRG neurite growth was reduced. Although our previous studies report increased DRG neurite growth with IL-4 alone (Gensel et al., 2009; Kigerl et al., 2009), those studies were performed using BM-derived macrophages and did not involve coculture. The results presented here are consistent with a previous study in which IL-4 treatment 2 h after LPS reduced nitric oxide production and motor neuron death beyond that of pretreatment with IL-4 (Zhao et al., 2006).

Increased neurite growth in the presence of inflammation is consistent with recent studies examining microglial activation in neurite development and axonal dieback. For example, DRG neurons cultured with conditioned media from BM-derived macrophages activated with zymosan (TLR-2/dectin-1 agonist) had increased axonal growth over baseline (Gensel et al., 2009). Moreover, pharmacological induction of inflammatory mediators (IL-1β, CCL2, and iNOS) protected against axonal dieback in a model of laser-induced SCI (IL-1β, CCL2, and iNOS; Stirling et al., 2014). Mice with attenuated inflammatory responses (i.e., TLR2^{KO} mice, minocycline treatment), however, had worse functional outcome after a contusive SCI (Kigerl et al., 2007; Stirling et al., 2014) and impaired axon regeneration after sciatic nerve injury (Kwon et al., 2013). Thus, an intact inflammatory response by microglia may be protective in the context of SCI.

Recruiting a specific macrophage population after SCI is another way in which IL-4 reprogramming of active microglia may be beneficial. Indeed, functional IL-4/IL-4Rα signaling in Adult-SCI mice corresponded to increased association of IL-4Rα$^+$ monocytes with the spinal cord, whereas the injured spinal cord of aged mice was dominated by IL-4Rα$^-$ macrophages. These results were mirrored in the immune-based studies wherein LPS-IL-4 treatment increased IL-1β and CCL2 expression corresponding with increased recruitment of CCR2$^+$/CX$_3$CR1^{lo}/IL-4Rα$^+$ macrophages to the brain. This CCR2$^+$/CX$_3$CR1^{lo}/IL-4Rα$^+$ phenotype is interpreted as beneficial for repair because CCR2$^+$/CX$_3$CR1^{lo} monocytes are characterized as iNOS^{lo} and associated with less pathology after SCI (Donnelly et al., 2011). Moreover, depletion of CCL2 is associated with reduced recovery after SCI (Shechter et al., 2009). CCL2 may be enhanced after IL-4 treatment as a result of increased polyamine levels. Arginase is the rate-limiting enzyme for production of polyamines, a necessary factor for CCL2 induction and macrophage recruitment to the brain (Puntambekar et al., 2011). Therefore, IL-4 signaling after SCI may be required for the recruitment or maintenance of a macrophage population that participates in repair. In further support of this idea, administration of an IL-4-expressing adenoviral vector into the CNS drives expression of chemokines to recruit other cells involved in immune regulation (i.e., regulatory T-cells) in a mouse model of multiple sclerosis (Butti et al., 2008).

In support of IL-4-driven recruitment of reparative macrophages, our experiments show that peripherally derived macrophages also developed an arginase$^+$ phenotype after LPS-IL-4 treatment. This arginase$^+$ phenotype is important because peripherally derived IL-4Rα$^+$/arginase$^+$ myeloid cells can function as myeloid derived suppressor cells (MDSCs; Bronte et al., 2003; Pesce et al., 2009; Kohanbash et al., 2013). Elimination of MDSC recruitment after SCI reduced arginase, IL-10, and IL-1β expression and caused worse functional recovery (Saiwai et al., 2013). It is unclear if peripherally derived IL-4Rα$^+$/arginase$^+$ myeloid cells exhibited here suppress T-cell responses consistent with MDSC function. Nonetheless, it is clear that IL-4 reprogramming of active microglia increases the association of CCR2$^+$/arginase$^+$ peripheral myeloid cells with the CNS.

In summary, inflammatory-induced IL-4Rα on microglia promoted increased sensitivity to IL-4 resulting in elevated arginase, IL-1β, and CCL2 expression and the recruitment of peripherally derived CCR2$^+$/IL-4Rα$^+$ cells to the CNS to benefit recovery after SCI. These data provide an innovative cellular perspective on IL-4 signaling and the pathophysiology of age-related deficits after CNS trauma.

References

Barrette B, Calvo E, Vallières N, Lacroix S (2010) Transcriptional profiling of the injured sciatic nerve of mice carrying the Wld(S) mutant gene: identification of genes involved in neuroprotection, neuroinflammation, and nerve regeneration. Brain Behav Immun 24:1254–1267. CrossRef Medline

Basso DM, Fisher LC, Anderson AJ, Jakeman LB, McTigue DM, Popovich PG

(2006) Basso Mouse Scale for locomotion detects differences in recovery after spinal cord injury in five common mouse strains. J Neurotrauma 23:635–659. CrossRef Medline

Bronte V, Serafini P, De Santo C, Marigo I, Tosello V, Mazzoni A, Segal DM, Staib C, Lowel M, Sutter G, Colombo MP, Zanovello P (2003) IL-4-induced arginase 1 suppresses alloreactive T cells in tumor-bearing mice. J Immunol 170:270–278. CrossRef Medline

Butovsky O, Ziv Y, Schwartz A, Landa G, Talpalar AE, Pluchino S, Martino G, Schwartz M (2006) Microglia activated by IL-4 or IFN-[gamma] differentially induce neurogenesis and oligodendrogenesis from adult stem/progenitor cells. Mol Cell Neurosci 31:149–160. CrossRef Medline

Butti E, Bergami A, Recchia A, Brambilla E, Del Carro UD, Amadio S, Cattalini A, Esposito M, Stornaiuolo A, Comi G, Pluchino S, Mavilio F, Martino G, Furlan R (2008) IL4 gene delivery to the CNS recruits regulatory T cells and induces clinical recovery in mouse models of multiple sclerosis. Gene Ther 15:504–515. CrossRef Medline

Cao Q, Xu XM, Devries WH, Enzmann GU, Ping P, Tsoulfas P, Wood PM, Bunge MB, Whittemore SR (2005) Functional recovery in traumatic spinal cord injury after transplantation of multineurotrophin-expressing glial-restricted precursor cells. J Neurosci 25:6947–6957. CrossRef Medline

Chen HY, Chen SS, Chiu WT, Lee LS, Hung CI, Hung CL, Wang YC, Hung CC, Lin LS, Shih YH, Kuo CY (1997) A nationwide epidemiological study of spinal cord injury in geriatric patients in Taiwan. Neuroepidemiology 16:241–247. CrossRef Medline

David S, Kroner A (2011) Repertoire of microglial and macrophage responses after spinal cord injury. Nat Rev Neurosci 12:388–399. CrossRef Medline

Donnelly DJ, Longbrake EE, Shawler TM, Kigerl KA, Lai W, Tovar CA, Ransohoff RM, Popovich PG (2011) Deficient CX3CR1 signaling promotes recovery after mouse spinal cord injury by limiting the recruitment and activation of Ly6Clo/iNOS+ macrophages. J Neurosci 31:9910–9922. CrossRef Medline

Fassett DR, Harrop JS, Maltenfort M, Jeyamohan SB, Ratliff JD, Anderson DG, Hilibrand AS, Albert TJ, Vaccaro AR, Sharan AD (2007) Mortality rates in geriatric patients with spinal cord injuries. J Neurosurg Spine 7:277–281. CrossRef Medline

Fenn AM, Henry CJ, Huang Y, Dugan A, Godbout JP (2012) Lipopolysaccharide-induced interleukin (IL)-4 receptor-alpha expression and corresponding sensitivity to the M2 promoting effects of IL-4 are impaired in microglia of aged mice. Brain Behav Immun 26:766–777. CrossRef Medline

Fenn AM, Gensel JC, Huang Y, Popovich PG, Lifshitz J, Godbout JP (2013) Immune activation promotes depression 1 month after diffuse brain injury: a role for primed microglia. Biol Psychiatry pii:S0006–3223(13)00950–5. CrossRef

Gensel JC, Nakamura S, Guan Z, van Rooijen N, Ankeny DP, Popovich PG (2009) Macrophages promote axon regeneration with concurrent neurotoxicity. J Neurosci 29:3956–3968. CrossRef Medline

Guerrero AR, Uchida K, Nakajima H, Watanabe S, Nakamura M, Johnson WE, Baba H (2012) Blockade of interleukin-6 signaling inhibits the classic pathway and promotes an alternative pathway of macrophage activation after spinal cord injury in mice. J Neuroinflammation 9:40. CrossRef Medline

Gwak YS, Hains BC, Johnson KM, Hulsebosch CE (2004) Locomotor recovery and mechanical hyperalgesia following spinal cord injury depend on age at time of injury in rat. Neurosci Lett 362:232–235. CrossRef Medline

Henry CJ, Huang Y, Wynne AM, Godbout JP (2009) Peripheral lipopolysaccharide (LPS) challenge promotes microglial hyperactivity in aged mice that is associated with exaggerated induction of both pro-inflammatory IL-1[beta] and anti-inflammatory IL-10 cytokines. Brain Behav Immun 23:309–317. CrossRef Medline

Huang Y, Henry CJ, Dantzer R, Johnson RW, Godbout JP (2008) Exaggerated sickness behavior and brain proinflammatory cytokine expression in aged mice in response to intracerebroventricular lipopolysaccharide. Neurobiol Aging 29:1744–1753. CrossRef Medline

Jakeman LB, Guan Z, Wei P, Ponnappan R, Dzwonczyk R, Popovich PG, Stokes BT (2000) Traumatic spinal cord injury produced by controlled contusion in mouse. J Neurotrauma 17:299–319. CrossRef Medline

Kigerl KA, McGaughy VM, Popovich PG (2006) Comparative analysis of lesion development and intraspinal inflammation in four strains of mice following spinal contusion injury. J Comp Neurol 494:578–594. CrossRef Medline

Kigerl KA, Lai W, Rivest S, Hart RP, Satoskar AR, Popovich PG (2007) Toll-like receptor (TLR)-2 and TLR-4 regulate inflammation, gliosis, and myelin sparing after spinal cord injury. J Neurochem 102:37–50. CrossRef Medline

Kigerl KA, Gensel JC, Ankeny DP, Alexander JK, Donnelly DJ, Popovich PG (2009) Identification of two distinct macrophage subsets with divergent effects causing either neurotoxicity or regeneration in the injured mouse spinal cord. J Neurosci 29:13435–13444. CrossRef Medline

Kitamura Y, Taniguchi T, Kimura H, Nomura Y, Gebicke-Haerter PJ (2000) Interleukin-4-inhibited mRNA expression in mixed rat glial and in isolated microglial cultures. J Neuroimmunol 106:95–104. CrossRef Medline

Kohanbash G, McKaveney K, Sakaki M, Ueda R, Mintz AH, Amankulor N, Fujita M, Ohlfest JR, Okada H (2013) GM-CSF promotes the immunosuppressive activity of glioma-infiltrating myeloid cells through interleukin-4 receptor-alpha. Cancer Res 73:6413–6423. CrossRef Medline

Kumar A, Stoica BA, Sabirzhanov B, Burns MP, Faden AI, Loane DJ (2013) Traumatic brain injury in aged animals increases lesion size and chronically alters microglial/macrophage classical and alternative activation states. Neurobiol Aging 34:1397–1411. CrossRef Medline

Kwon MJ, Kim J, Shin H, Jeong SR, Kang YM, Choi JY, Hwang DH, Kim BG (2013) Contribution of macrophages to enhanced regenerative capacity of dorsal root ganglia sensory neurons by conditioning injury. J Neurosci 33:15095–15108. CrossRef Medline

Lee DC, Ruiz CR, Lebson L, Selenica ML, Rizer J, Hunt JB Jr, Rojiani R, Reid P, Kammath S, Nash K, Dickey CA, Gordon M, Morgan D (2013) Aging enhances classical activation but mitigates alternative activation in the central nervous system. Neurobiol Aging 34:1610–1620. CrossRef Medline

Lee SI, Jeong SR, Kang YM, Han DH, Jin BK, Namgung U, Kim BG (2010) Endogenous expression of interleukin-4 regulates macrophage activation and confines cavity formation after traumatic spinal cord injury. J Neurosci Res 88:2409–2419. CrossRef Medline

Lyons A, Griffin RJ, Costelloe CE, Clarke RM, Lynch MA (2007) IL-4 attenuates the neuroinflammation induced by amyloid-β in vivo and in vitro. J Neurochem 101:771–781. CrossRef Medline

Mosser DM, Edwards JP (2008) Exploring the full spectrum of macrophage activation. Nat Rev Immunol 8:958–969. CrossRef Medline

National SCI Statistical Center (2013) Facts and figures at a glance. Birmingham, AL: University of Alabama at Birmingham.

Norden DM, Fenn AM, Dugan A, Godbout JP (2014) TGFβ produced by IL-10 re-directed astrocytes attenuates microglial activation. Glia 62:881–895. CrossRef Medline

Onyszchuk G, He YY, Berman N, Brooks WM (2008) Detrimental effects of aging on outcome from traumatic brain injury: a behavioral, magnetic resonance imaging, and histological study in mice. J Neurotrauma 25:153–171. CrossRef Medline

Pesce JT, Ramalingam TR, Mentink-Kane MM, Wilson MS, El Kasmi KC, Smith AM, Thompson RW, Cheever AW, Murray PJ, Wynn TA (2009) Arginase-1-expressing macrophages suppress Th2 cytokine-driven inflammation and fibrosis. PLoS Pathog 5:e1000371. CrossRef Medline

Popovich PG, Wei P, Stokes BT (1997) Cellular inflammatory response after spinal cord injury in Sprague-Dawley and Lewis rats. J Comp Neurol 377:443–464. CrossRef Medline

Puntambekar SS, Davis DS, Hawel L 3rd, Crane J, Byus CV, Carson MJ (2011) LPS-induced CCL2 expression and macrophage influx into the murine central nervous system is polyamine-dependent. Brain Behav Immun 25:629–639. CrossRef Medline

Saiwai H, Kumamaru H, Ohkawa Y, Kubota K, Kobayakawa K, Yamada H, Yokomizo T, Iwamoto Y, Okada S (2013) Ly6C+Ly6G- Myeloid-derived suppressor cells play a critical role in the resolution of acute inflammation and the subsequent tissue repair process after spinal cord injury. J Neurochem 125:74–88. CrossRef Medline

Sandhir R, Onyszchuk G, Berman NE (2008) Exacerbated glial response in the aged mouse hippocampus following controlled cortical impact injury. Exp Neurol 213:372–380. CrossRef Medline

Shechter R, London A, Varol C, Raposo C, Cusimano M, Yovel G, Rolls A, Mack M, Pluchino S, Martino G, Jung S, Schwartz M (2009) Infiltrating blood-derived macrophages are vital cells playing an anti-inflammatory

role in recovery from spinal cord injury in mice. PLoS Med 6:e1000113. CrossRef Medline

Shechter R, Miller O, Yovel G, Rosenzweig N, London A, Ruckh J, Kim KW, Klein E, Kalchenko V, Bendel P, Lira SA, Jung S, Schwartz M (2013) Recruitment of beneficial M2 macrophages to injured spinal cord is orchestrated by remote brain choroid plexus. Immunity 38:555–569. CrossRef Medline

Siegenthaler MM, Berchtold NC, Cotman CW, Keirstead HS (2008) Voluntary running attenuates age-related deficits following SCI. Exp Neurol 210:207–216. CrossRef Medline

Sierra A, Gottfried-Blackmore AC, McEwen BS, Bulloch K (2007) Microglia derived from aging mice exhibit an altered inflammatory profile. Glia 55:412–424. CrossRef Medline

Sroga JM, Jones TB, Kigerl KA, McGaughy VM, Popovich PG (2003) Rats and mice exhibit distinct inflammatory reactions after spinal cord injury. J Comp Neurol 462:223–240. CrossRef Medline

Stirling DP, Cummins K, Mishra M, Teo W, Yong VW, Stys P (2014) Toll-like receptor 2-mediated alternative activation of microglia is protective after spinal cord injury. Brain 137:707–723. CrossRef Medline

Wohleb ES, Hanke ML, Corona AW, Powell ND, Stiner LM, Bailey MT, Nelson RJ, Godbout JP, Sheridan JF (2011) [Beta]-adrenergic receptor antagonism prevents anxiety-like behavior and microglial reactivity induced by repeated social defeat. J Neurosci 31:6277–6288. CrossRef Medline

Wohleb ES, Fenn AM, Pacenta AM, Powell ND, Sheridan JF, Godbout JP (2012) Peripheral innate immune challenge exaggerated microglia activation, increased the number of inflammatory CNS macrophages, and prolonged social withdrawal in socially defeated mice. Psychoneuroendocrinology 37:1491–1505. CrossRef Medline

Wohleb ES, Powell ND, Godbout JP, Sheridan JF (2013) Stress-induced recruitment of bone marrow-derived monocytes to the brain promotes anxiety-like behavior. J Neurosci 33:13820–13833. CrossRef Medline

Xu H, Chen M, Manivannan A, Lois N, Forrester JV (2008) Age-dependent accumulation of lipofuscin in perivascular and subretinal microglia in experimental mice. Aging Cell 7:58–68. CrossRef Medline

Zhao W, Xie W, Xiao Q, Beers DR, Appel SH (2006) Protective effects of an anti-inflammatory cytokine, interleukin-4, on motoneuron toxicity induced by activated microglia. J Neurochem 99:1176–1187. CrossRef Medline